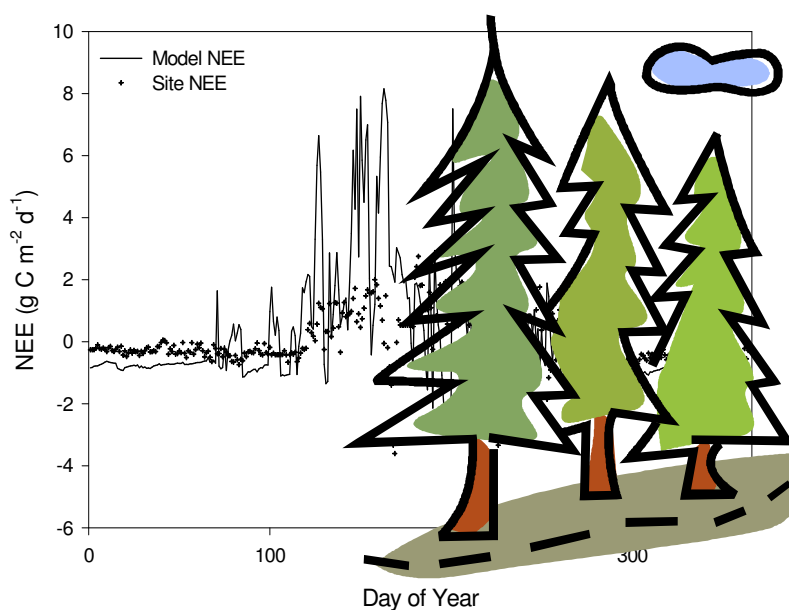MPI-BGC

Jena

TECHNICAL REPORTS
16

PARAMETER ESTIMATION AND VALIDATION OF THE
TERRESTRIAL ECOSYSTEM MODEL BIOME-BGC
USING EDDY-COVARIANCE FLUX MEASUREMENTS

by
Kristina Trusilova, James Trembath and Galina Churkina

Technical Reports - Max-Planck-Institut für Biogeochemie 16, 2009

PARAMETER ESTIMATION AND VALIDATION OF THE TERRESTRIAL ECOSYSTEM MODEL BIOME-BGC USING EDDY-COVARIANCE FLUX MEASUREMENTS

Kristina Trusilova, James Trembath, and Galina Churkina

Max-Planck Institute for Biogeochemistry

07745, Jena, Germany

Contributors:

Vetter M.[1], Reichstein M.[1,1,2], Schumacher J.[1,3], Knohl A.[1,4], Rannik U.[5], Gruenwald T.[6], Moors E.[7], Granier A.[8]

[1] Dept. of Forest Environment and Resources, DISAFRI, University of Tuscia, I-01100 Viterbo, Italy

[2] Potsdam Institute for Climate Impact Research, Telegrafenberg C4, D-14473 Potsdam, Germany

[3] Institute of Ecology, University of Jena, Germany

[4] University of California, ESPM Dept., Ecosystem Science Division, 151 Hilgard #3110, Berkeley, CA 94705-3110, USA

[5] Department of Physics, University of Helsinki , P.O.BOX 9 FIN-00014 Helsinki, Finland

[6] Technische Universität Dresden Institut für Hydrologie und Meteorologie D-01062 Dresden, Germany

[7] Alterra, P.O. Box 47, NL-6700 AA Wageningen, The Netherlands

[8] Unité Ecophysiologie, INRA-Nancy, F-54280 Champenoux, France

Content

PARAMETER ESTIMATION FOR THE TERRESTRIAL ECOSYSTEM MODEL BIOME-BGC USING EDDY-COVARIANCE FLUX MEASUREMENTS   38

Abstract

Predictive capacity of a numerical model is determined by model structure as well as model parameters. To make reliable model predictions we have to show that model can replicate observations or, in other words, model has to be validated. During the model validation the parameters of the model are usually adjusted to achieve a better fit of modelled and observed variables. Parameters can be adjusted either manually by user or automatically by a computer program.

In this report we use observations of CO_2 fluxes measured with the eddy covariance technique first, to validate the terrestrial ecosystem model BIOME-BGC and then to optimize model parameters for several forest sites.

In the first chapter we presents validation of net ecosystem exchange, gross primary production, and respiration simulated by BIOME-BGC for 10 sites located in four northern-hemispheric forest biomes, where CO_2 flux measurements have been made under the FLUXNET (AMERIFLUX[9] and EUROFLUX[10]) program, at the inter-annual, annual, intra-annual, and daily levels. We show that model works better for temperate than for boreal forests. Inclusion of multiple soil layers in the model instead of one bucket algorithm could help to improve the model performance especially in the North. Modelled respiration rate was higher than observed at low temperatures, but in good agreement at high temperatures.

In the second chapter we estimate model parameters using optimisation routine, which is based on the Metropolis algorithm, and observations from six forest sites. In addition to carbon flux measurements we use also observations of leaf area index. We demonstrate that a more accurate estimation of model parameters helps to reduce the uncertainty in the model output – the estimates of carbon fluxes. The retrieved values of model parameters provide a reduction of an average flux uncertainty by 60%-80% over the modelled time period (year 2001). The largest reduction of flux and parameter uncertainties was achieved with the largest number of constraints on the model output for five sites and with the single constraint on the ecosystem respiration for Hesse. The new parameter estimates provided also a reduction of the flux uncertainty at two additional sites that were not included into the optimisation.

---

[9] http://public.ornl.gov/ameriflux/

[10] http://www.unitus.it/dipartimenti/disafri/progetti/eflux/euro.html

Introduction

The terrestrial ecosystems together with the marine environments limit atmospheric CO_2 concentrations and, consequently, the extent of the climate change. However, the estimates of the terrestrial carbon budget are uncertain, with the uncertainty amounted to 2-4 Gt C per year for the 1990's (Schimel et al., 2001). The uncertainties originate not only from the complex responses of terrestrial ecosystems to environmental drivers, but also from our observational system of the carbon cycle. Available methods to measure various components of the carbon budget over large areas (e.g. global atmospheric CO_2 sampling network, process studies, satellite observations, etc.) provide insights into certain components of the terrestrial carbon budget, but none of them supplies complete information about all components. Moreover they provide information about different components of the carbon cycle at different spatial and temporal scales, so using these methods in a complementary way is not straightforward and the resulting carbon budget is ambiguous.

Ecosystem models serve as integrative tools for observations because they estimate relevant components of the carbon cycle at different spatial and temporal scales. A number of ecosystem terrestrial models: TURC (Ruimy et al., 1996), BETHY (Knorr, 2000), LPJ (Sitch et al., 2003), BIOME3 (Haxeltine and Prentice, 1996), PnET (Aber and Federer, 1992), BIOME-BGC (Running and Hunt, 1993; Thornton, 1998; Thornton et al., 2002)) were developed to estimate carbon cycle variables in the terrestrial biosphere. However estimates of the carbon variables still have uncertainties related to poorly understood links between "slow" (e.g. allocation, soil decomposition, etc.) and "fast" processes (e.g. photosynthesis, respiration, evapotranspiration) as well as to internal parameters and pools (e.g. leaf, stem, and soil carbon), which have not been properly constrained by observations.

In the first part we presents validation of net ecosystem exchange, gross primary production, and respiration simulated by BIOME-BGC for 10 sites located in four northern-hemispheric forest biomes, where CO_2 flux measurements have been made under the FLUXNET (AMERIFLUX[11] and EUROFLUX[12]) program, at the inter-annual, annual, intra-annual, and daily levels.

In the second part we estimate model parameters using optimisation routine, which is based on the Metropolis algorithm, and observations from six forest sites. In addition to carbon flux

---

[11] http://public.ornl.gov/ameriflux/

[12] http://www.unitus.it/dipartimenti/disafri/progetti/eflux/euro.html

measurements we use also observations of leaf area index. We investigate which observations or which combinations of them better constrain the model parameters and which model parameters are the most critical ones for the improvement of carbon flux estimates. Finally we test if our approach is suitable for development of a general forest parameterisation which can be applied to simulate regional or continental carbon budgets.

Model Description

The BIOME-BGC model simulates the storage and fluxes of water, carbon, and nitrogen within the vegetation, litter, and soil components of a terrestrial ecosystem. Much of the fundamental logic for BIOME-BGC springs from the FOREST-BGC family of models (Running and Coughlan, 1988; Running and Hunt, 1991; Running, 1994). The BIOME-BGC model is an extended version for use with different vegetation types, which may be identified and partially characterised by remote sensing methods. The basic structure of the model incorporates the long-term experience of established forest ecosystem scientists (Waring and Running, 1998), and at the same time has been modified for spatial simulations, i.e. is prepared for use in a landscape or regional context.

The model structure is based on some key simplifying assumptions that have proved to be particularly valuable in extending ecosystem analyses to regional levels. Trees are not defined individually as in a typical forest stand growth model. The cycling of carbon, water and nitrogen are expressed in mass units. Species are also not explicitly identified, although species-specific physiological characterisation can be represented. Geometric complexities of different tree canopies are reduced to a simple quantification of the sum of all leaf layers as leaf area index. All biogeochemical processes are simulated within the vertical extent of a vegetation canopy and its rooting system. For computational convenience and keeping model parameters and outputs dimensionally consistent with observations, an arbitrary unit of horizontally projected area is defined, over which all fluxes and storage are quantified. Complete horizontal homogeneity is assumed within that unit area. This horizontal area and the vertical extent of the canopy and its rooting system define the maximum physical boundaries of the simulation system. This includes all living and dead plant materials, leaf or shoot boundary layer, the litter and soil surfaces, all mineral and organic matters making up the soil and litter down to a depth at which root penetration is negligible, all water held in the soil down to that same depth, and any snow cover.

The temporal framework of the BIOME-BGC model (version 4.1.1) consists of a dual discrete time step approach, which is slightly different from the implementation in previous versions of the BGC logic (Running and Hunt, 1993; Hunt et al., 1996). In the latest version of the BIOME-BGC most simulated ecosystem activity occurs at a daily time step, driven by daily values for maximum and minimum temperatures (*Tmax*, *Tmin*), precipitation (*Precip*), solar radiation (*SRad*), and air humidity (*RHum*). Examples of daily processes are soil water balance, photosynthesis, allocation, litterfall, and carbon and nitrogen dynamics in the litter and soil. Phenological timing of the budburst is determined once a year using long-term

thermal sums and soil moisture status for deciduous forests and grasslands (White et al., 1997). For evergreen vegetation, current climatic conditions determine the beginning and the end of growing season.

Finally, the model is designed to require only standard meteorological data, namely, daily maximum-minimum temperature, precipitation, incoming shortwave solar radiation, vapour pressure deficit (*VPD*), and the day length (*DLn*), so that the model may be applied beyond those sites with sophisticated instrumentation.

In this study, we used BIOME-BGC to simulate daily net ecosystem productivity, gross photosynthesis, ecosystem respiration, and projected leaf area index (*LAI*). *Net Ecosystem Production* (*NEP*) was computed as a difference between gross photosynthesis and respiration (autotrophic and heterotrophic). *Gross Photosynthetic Production* (*GPP*) was calculated based on absorbed photosynthetically active radiation, atmospheric carbon dioxide concentration, air temperature, vapour pressure deficit, precipitation, atmospheric nitrogen deposition, the leaf area index, and available nitrogen content in soil. Finally:

$$NEP = GPP - RESP$$

Ecosystem RESPiration (RESP) was a sum of autotrophic and heterotrophic respirations. *Autotrophic Respiration* was a sum of maintenance and growth respiration of different parts of plant (canopy, stem, roots). Maintenance respiration of each plant compartment was computed as a function of compartment's nitrogen content and temperature. Growth respiration was calculated on the basis of construction costs by plant compartment. Different construction costs were applied to woody and non-woody plant tissues. *Heterotrophic respiration* included decomposition of both litter and soil and was related to their chemical composition (cellulose, lignin, and humus), to their carbon to nitrogen ratios, to soil mineral nitrogen availability and to soil moisture and temperature. Thus, BIOME-BGC was able to simulate effects of a number of abiotic (temperature, vapour pressure deficit, soil water, solar radiation, atmospheric CO_2 concentration, and atmospheric nitrogen deposition) and biotic (leaf area index, soil carbon and nitrogen contents) controls on net carbon flux. Ecosystem respiration is calculated as:

$$RESP = Autotrophic\ Respiration + Heterotrophic\ Respiration$$
$$Autotrophic\ Respiration = Maintenance\ Respiration + Growth\ Respiration$$

Vegetation composition in the BIOME-BGC model is described by seven different vegetation types defined within the model by ecophysiological parameters (Table 1).

Table 1. Ecophysiological parameterisation for all broadleaf deciduous and evergreen needleleaf forests.

Parameter		Unit	Description
DBF	ENF		
*	*	DIM	Transfer growth period as fraction of growing season
*	*	DIM	Litterfall as fraction of growing season
1.0	0.26	1/yr	Annual leaf and fine root turnover fraction
0.7	0.7	1/yr	Annual live wood turnover fraction
0.005	0.005	1/yr	Annual whole-plant mortality fraction
0.0025	0.005	1/yr	Annual fire mortality fraction
1.0	1.4	DIM	(ALLOCATION) ratio of new fine root C to new leaf C
2.2	2.2	DIM	(ALLOCATION) ratio of new stem C to new leaf C
0.1	0.071	DIM	(ALLOCATION) ratio of new live wood C to new total wood C
0.23	0.29	DIM	(ALLOCATION) ratio of new root C to new stem C
0.5	0.5	DIM	(ALLOCATION) ratio of current growth proportion to storage growth
24	42	kgC/kgN	C:N of leaves
49	93	kgC/kgN	C:N of leaf litter, after re-translocation
42	58	kgC/kgN	C:N of fine roots
50	50	kgC/kgN	C:N of live wood
442	730	kgC/kgN	C:N of dead wood
0.39	0.31	DIM	Leaf litter labile proportion
0.44	0.45	DIM	Leaf litter cellulose proportion
0.17	0.24	DIM	Leaf litter lignin proportion
0.30	0.34	DIM	Fine root labile proportion
0.45	0.44	DIM	Fine root cellulose proportion
0.25	0.22	DIM	Fine root lignin proportion
0.76	0.71	DIM	Dead wood cellulose proportion
0.24	0.29	DIM	Dead wood lignin proportion
$5 \cdot 10^{-5}$	$2.5 \cdot 10^{-5}$	1/LAI/day	Canopy water interception coefficient
0.7	0.51	DIM	Canopy light extinction coefficient
2.0	2.6	DIM	All-sided to projected leaf area ratio
30.0	8.2	m^2/kgC	Canopy average specific leaf area (projected area basis)
2	2	DIM	Ratio of shaded SLA : sunlit SLA
0.08	0.07	DIM	Fraction of leaf N in Rubisco
0.005	0.006	m/s	Maximum stomata conductance (projected area basis)
$1 \cdot 10^{-5}$	$6 \cdot 10^{-5}$	m/s	Cuticular conductance (projected area basis)
0.01	0.09	m/s	Boundary layer conductance (projected area basis)
−0.60	−0.63	Mpa	Leaf water potential : start of conductance reduction
−2.3	−2.3	Mpa	Leaf water potential : complete conductance reduction
930	610	Pa	Vapour pressure deficit : start of conductance reduction
4100	3100	Pa	Vapour pressure deficit : complete conductance reduction

* These two parameters determine the duration of the transfer growth and litter fall periods, the constants used were defined by for each biome.

Model updates

Two important changes were made to the benchmark v4.1.1 of the model. Firstly the simplified logic of N deposition rate over time was changed so that the N deposition was no longer scaled according to the changes in CO_2 concentration but was independent. This allowed for non-linear resolution of N deposition over time (Figure 1).
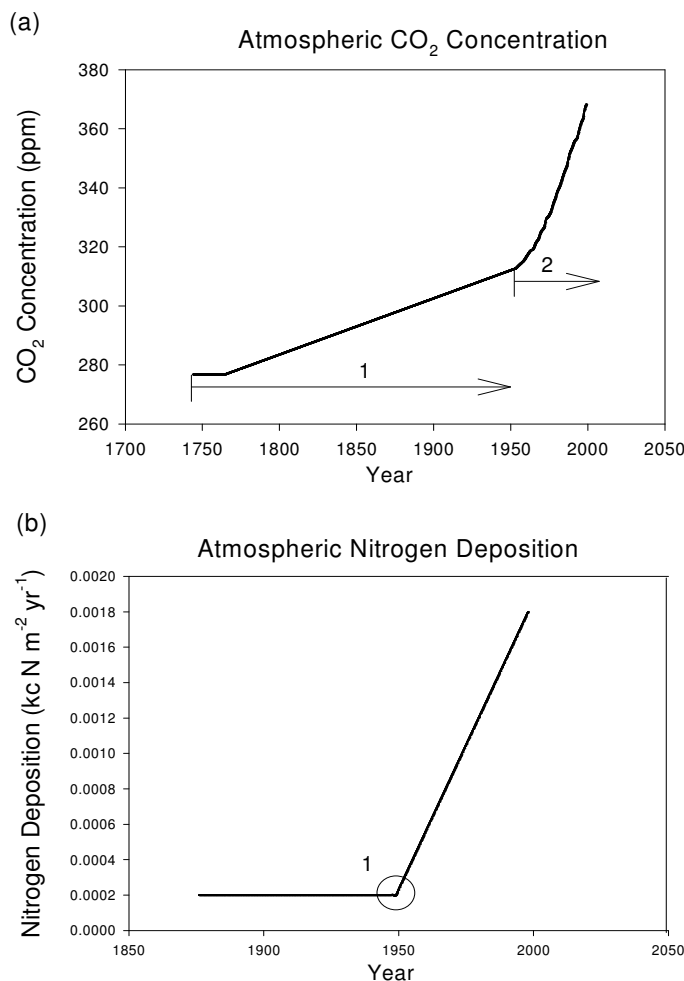
Figure 1. Representation of the carbon dioxide concentration in the atmosphere (a) for input to Biome-BGC, span 1, data from the Siple Ice Core, span 2, data from atmospheric measurements (Manua Loa). Simplification of historical nitrogen deposition (b) for input to Biome-BGC, point 1 being the transition point the historical background values to those influenced by man after the discovery of the Haber-Bosch process.

The logic determining the translocation of leaf N in the spring was changed, from the logic of v4.1.1 back to that of v4.1. The underlying reasons for this change were the polarised

logics of the two versions. V4.1 can be considered a recipient based flow, the deployment of re-translocated leaf N in the spring is based on the requirement of the plant, and access by the plant to this pool was ungoverned. This often resulted in an initial modelled *Net Ecosystem Exchange* (*NEE*) spike in the early growing season, something that is often seen in the carbon flux data, especially for temperate coniferous species under high N deposition rates. However, V4.1.1 can be considered as a donor based flow, in that the deployment of the re-translocated leaf N in the spring is a fractionation of the initial size of the translocated pool at the end of the previous growing season, not a translation in any way of plant demand. In test simulations this induced the long-term build up of N, inaccessible to the plant, conceptually turning the re-translocated pool into a permanent N sink. The translation of this logic to the overall modelled *NEE* flux was to induce a mid-season crash in productivity as a result of N deficiency, something not seen in the EUROFLUX data.

Modelling four forest biome types using a process based ecophysiological model BIOME-BGC: validation and uncertainties

By James Trembath and Galina Churkina

Objectives

The BIOME-BGC model and its predecessors have been validated for many different ecological forest variables in the US (Running and Coughlan, 1988; Turner et al., 1996; Hunt et al., 1999) and in Europe (Pietsch and Hasenauer, 2002; Merganicova et al., 2005; Pietsch et al., 2005; Vetter et al., 2005; Cienciala and Tatarinov, 2006; Tatarinov and Cienciala, 2006; Petritsch et al., 2007). Testing of the modeled CO_2 and water fluxes has been done for certain forest types in the US (Kimball et al., 1997; Thornton et al., 2002) and in Europe (Cienciala et al., 1998b; Cienciala and Lindroth, 1999; Churkina et al., 2003).

This study presents comprehensive validation of *NEE, GPP* and *RESP* simulated by BIOME-BGC for 10 sites located in four northern-hemispheric forest biomes, where CO_2 flux measurements have been made under the FLUXNET program, at the inter-annual, annual, intra-annual and daily levels.

Site characteristics and meteorological data

This study covers ten sites at four northern-hemispheric forest biomes where CO_2 flux measurements have been made under the FLUXNET program. These sites cover a range of climates, with an annual average temperature from

–0.36°C to +11.4°C and annual total precipitation in the range of 48-110 cm (Figure 2).
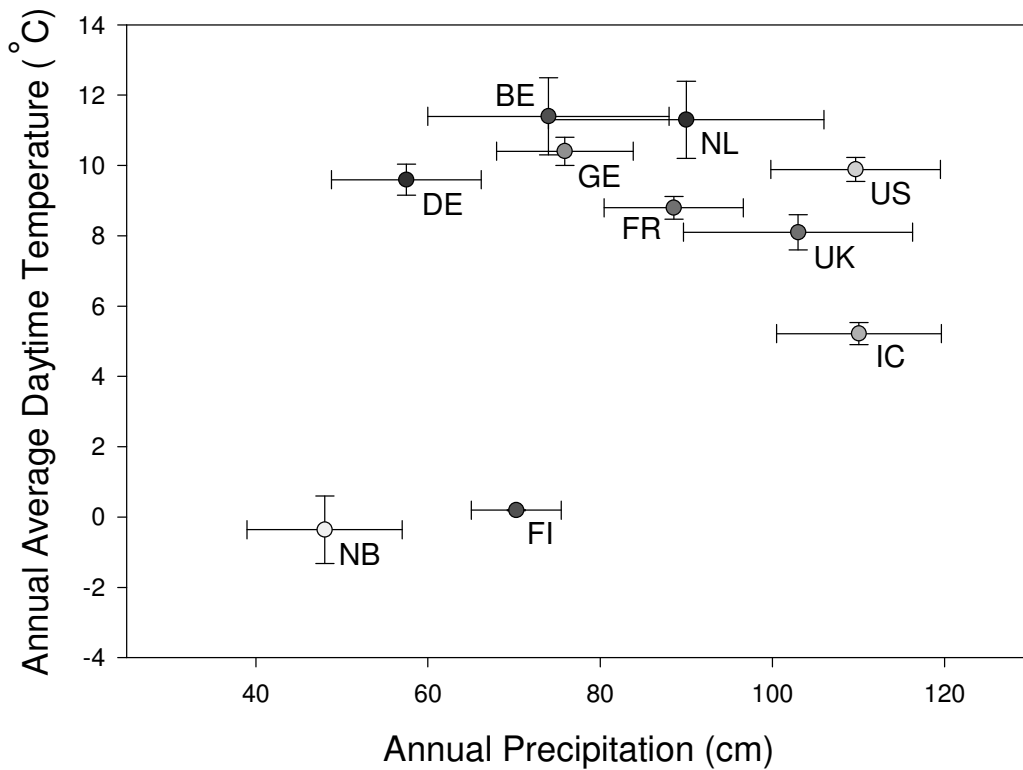
Figure 2. Study sites ordered by climate characteristics: annual average temperature [°C], total annual precipitation [cm], and their standard deviations for the ten sites modelled.

The site characteristics needed for the parameterisation in the model are listed in Table 2 and Table 3. These tables also give the site codes and biome types that were used in this study. The following descriptions allude to the origin of the data in the tables and any subsequent data that may be of interest.

Table 2. Site-specific parameters[13].

Site code	Site name/country	Lat	Lon	Elevation [m]	Soil Texture [%]			Soil depth [m]	N dep. [kg N ha^{-1}]
					sand	silt	clay		
DK	Soroe/Denmark	55°29′	11°38′	40	54	32	14	0.5-2.5	18 *
FR	Hesse/France	48°40′	07°03′	305	6	67	27	1.5	20
US	Harvard/USA	42°03′	72°00′	340	54	38	8	1.0	8 **
NB	North Boreas/CA	55°80′	-97°84′	218	31	29	40	0.4	2 ***
FI	Hyytiala/Finland	61°51′	24°17′	170	70	20	10	0.4	4 #
IC	Gunnarsholt/Iceland	63°05′	-20°13′	78	61	32	7	0.8	46 ##
BE	Brasschaat/Belgium	51°18′	04°31′	16	93	5	2	1.8-2.3	40
GE	Tharandt/Germany	50°58′	13°38′	380	20.7	41.4	37.9	1.5	30
NL	Loobos/Netherlands	52°10′	05°44′	25	96	2	2	0.5	40
UK	Aberfeldy/UK	56°37′	-03°48′	340	43	31	26	0.7	65 ###

* - The nitrogen deposition was estimated at 40 kg N ha^{-1}y^{-1} from another beech stand in Denmark, part of the ICP Forests of UN-ECE (International Co-operative Programme on Assessment and Monitoring of Air Pollution Effects on Forests

** - The nitrogen deposition rate is 8.8 kg N ha^{-1}y^{-1} (Munger et al., 1998)

*** - The nitrogen deposition for the site was unknown and assumed to be at a base level

\# - The nitrogen deposition is approximately 40 kg N ha^{-1} y^{-1} (Kulmala et al., 1998a)

\#\# - Agricultural applications of nitrogen whilst the site was a hayfield were in the order 100 kg N ha^{-1} yr^{-1} (J. Guðmundsson, *personal communication*), silivicultural nitrogen application also occurred after planting but at an unknown rate, the magnitude of this application was assumed to be similar to that of Aberfeldy

\#\#\# - The management strategy for N fertilisation is a 10 plot, with 10 year rotations of N application within the catchment. It was assumed for ease that this was applied in one catchment wide application of 350 kg N ha^{-1} y^{-1} every 10 years (J. Moncreiff, *personal communication*). It was also assumed that the silvicultural application rate would decay over time. This decay rate was assigned at 20% of the previous years N (Bormann et al., 1977).

The model requires maximum *(Tmax, ℃)*, minimum (*Tmin, ℃*), and daylight average temperature (°C), as well as precipitation (*Precip*, cm), vapour pressure deficit (*VPD*, Pa), solar short-wave radiation (*SRad*, W m^{-2}) and day length (*DLen,* sec), as driving meteorological variables. The long-term meteorology data used to drive the model in this study were drawn from different resources namely synoptic meteorology stations and the HadCM2 GCM[14].

---

[13] N.B. N depositions are for 1998, Gunnarsholt and Aberfeldy had direct application of nitrogen fertilizers

[14] www.ipcc-data.org/is92/hadcm2_info.html

The meteorological site data used to drive the model for the analyses was taken directly from the meteorological stations in situ at the flux towers or stations near the tower. The data received was of differing quality and length. Small scale gaps, in the region of days, were filled by taking the mean of the surrounding days. Years in which large data gaps were present for any one variable were removed from the analysis. If any of these variables were unavailable for any site they were estimated using the climate simulator MT-CLIM (Mountain Microclimate Climate Simulator) model (Running et al., 1987; Glassy and Running, 1994).

Table 3. Biome types, vegetation age, and dominant species at the chosen sites.

Site code	DK	FR	US	NB	FI	IC	BE	GE	NL	UK
Biome Type	Temp Decid	Temp Decid	Temp Decid	Boreal Conif	Boreal Conif	Boreal Decid	Temp Conif	Temp Conif	Temp Conif	Temp Conif
Forest age in 2000	83	35	73	100	38	12	73	99	83	20
Species	Beech	Beech	Mixed Decid	Old Black Spruce	Scots Pine	Black Cotton -wood	Scots Pine	Norway Spruce	Scots Pine	Sitka Spruce
Young Plant	3	3	10	4	4	2	4	8.8	4	4
Transfer periods	0.1 0.9	0.1 0.9	0.1 0.9	0.3 0.3	0.3 0.3	0.3 0.3	0.3 0.3	0.3 0.3	0.3 0.3	0.3 0.3

Temperate deciduous forest sites

Soroe (Denmark, DK). Soroe is a stand of European beech (*Fagus sylvatica* L.) on the Danish Island of Zealand, the terrain is flat and there is a homogeneous fetch of 500-2000 m. Before bud-break the understory vegetation is composed mainly of wood anemone (*Anemone nemorosa* L.) and dog's mercury (*Mercurialis perennis* L.), later in the growing season only patches of grass survive the low light conditions. There are scattered stands of conifers, approximately 20% of the footprint area, predominantly Norway spruce (*Piceas abies* (L.) Karst.) and single trees of European larch (*Larix decidua* Mill.). The soil is a mollisol with a deep organic layer up to 40 cm deep (Pilegaard et al., 2001).

The long-term meteorological data were taken from the Landbohøjskolen meteorological station of the Danish Meteorological Institute, 55°41'N 12°32'E, at an altitude of 9 m. The data were complete from 1874 to 1997 for *Tmax*, *Tmin*, and *Precip*.

Hesse (France, FR). Hesse forest is a stand composed of 90% Beech (*Fagus sylvatica* L.). Other species in the stand include European hornbeam (*Carpinus betulus* L.), silver birch (*Betula pendula* B.), sessile oak (*Quercus petraea* Matt.), and European larch (*Larix decidua* Mill.). There is very little understory vegetation and the soil type is an intermediate between a luvisol and a stagnic luvosol (Granier et al., 2000).

The meteorology data for Hesse came from two meteorological stations of Meteo France. Precipitation came from Sarrebourg, close to the Hesse forest (approximately 5 km North), 48°44' N 7°04'E at an elevation of 254 m. *SRad*, *Tave*, and *VPD* came from the Danne et Quatre Vents meteorology station, 48°46'N 7°17'E, 350 m. *Tmax* and *Tmin* data were calculated from the best of an ensemble of multiple regressions of contemporary data from these two stations (Figure 3).

The plot shows the regression equation:

$$y = 4.53 + 0.016 \cdot x_1 + 0.0035 \cdot x_2$$
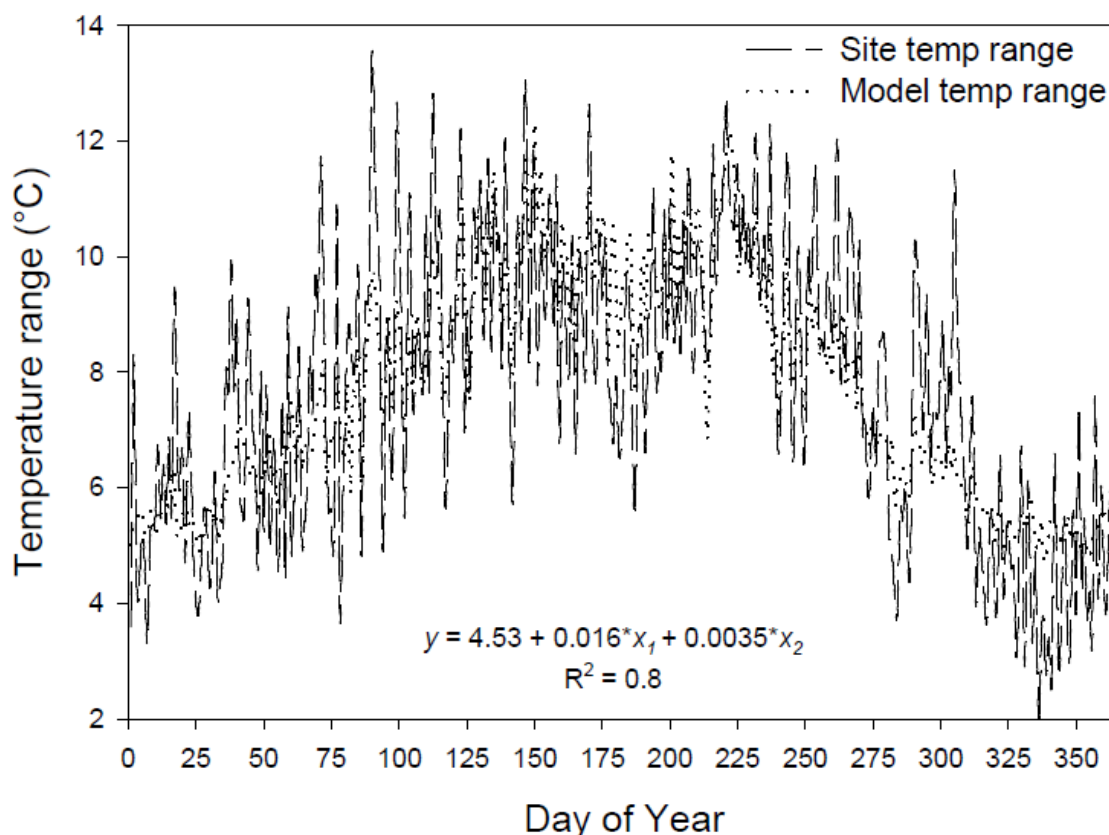$$R^2 = 0.8$$

Figure 3. Daily temperature ranges for Hesse site averaged over 1997, 1998, 1999 and the results of a regression model with the two independent variables of radiation and VPD used to estimate the temperature ranges for the Hesse long-term meteorological data set.

Harvard (USA, US). The measurements for the Harvard site were made on the Prospect Hill tract of the Harvard forest, Massachusetts. The forest is of mixed species - dominated by red oak (*Quercus rubra* L.) and red maple (*Acer rubrum* L.) with scattered stands of hemlock (*Tsuga canadensis* L.) and white and red pine (*Pinus strobus* L., *Pinus resinosa* Ait.) - and mixed ages between 50 and 80 years old (Goulden et al., 1996).

Tmin, *Tmax*, and 24-hour *Precip* amounts were recorded daily at NOAA's Shaler Meteorological station, 42°53′N −72°19′E, at an elevation of 340 m. The meteorological data is continuous from 1964 to 2001.

Boreal coniferous forest sites

North Boreas (Canada, NB). The Northern Study Area (BOREAS) is 100×80 km around Thompson, Manitoba, Canada. It is quite typical of the extreme northern boreal forest. It is gentle in terrain, contains few lakes and is covered primarily with black spruce (*Picea mariana* Mill.), scattered birch and some stands of jack pine *(Pinus banksiana* Lamb.). There is very little aspen, occurring only in very small patches (Newcomer et al., 2000).

The long-term meteorological data used in the north BOREAS simulations were extracted from the NCDC Summary of the Day database for the meteorological station at Thompson Airport, Manitouba, Canada, 55°52'N −97°55'E at an elevation of 218 m. *Tmax*, *Tmin*, *Tave*, and *Precip* data were continuous from 1975 to 1997; days with missing data were filled by taking the mean of the surrounding days.

Hyytiala (Finland, FI). Hyytiala site has a homogeneous Scots pine (*Pinus sylvestris* L.) dominated stand. 1% of the forested area is downy birch (*Betula pubescencs* Ehrh.), grey alder (*Alnus incana* Moench), and aspen (*Populus tremula* L.). The ground cover is a mixture of heather (*Calluna vulgaris* L.), lingonberry (*Vaccinium vitis-idaea* L.) and blueberry (*V.myrtillus* L.). The terrain has modest height variations and the soil is a haplic podzol with a parent material of coarse, silty, glacial till (Vesala et al., 2000).

The meteorology data was taken from the Finnish Meteorological Institutes station located near the flux site. The data for *Tmax*, *Tmin*, *Tave*, *Precip*, and *RHum* were available. Values for *SRad* were also available from the Hyytiala meteorological station from 1983 to 2000.

Boreal deciduous forest sites

Gunnarsholt (Iceland, IC). In 1989, the existing hayfield was stripped of its sod, leaving essentially bare soil with some strips of grass. The site was then planted with black cottonwood (*Populus trichocarpa* Torr. & Grey)(Aradottir et al., 1997).

Tmax, *Tmin*, *Tave*, *Precip*, and *VPD* were taken for the period 1958 to 2000 from the Hella meteorology station, 63°50′N −20°24′E, 20 m elevation, of the Icelandic Meteorological Office. Gaps in this data were minimal, missing temperature and precipitation data accounting for only 564 data gap days and were substituted with data from another station Haell, 64°04′N −20°15′E, at 121 m.

Temperate coniferous forest sites

Brasschaat (Belgium, BE). Brasschaat, is located in the province of Antwerpen, the forest is predominantly Scots pine (*Pinus sylvestris* L.), with patches of English oak (*Quercus robur* L). The understory layer is either wild black cherry (*Prunus serotina* J.F. Ehrh) and rhododendron (*Rhododendron ponticum* L.) or a ground covering of purple moor grass (*Molina caerulea* (L.) Moench.) (Gond et al., 1999).

The meteorological fields for Braaschaat were simulated using climate data from CRU[15] with climate change impacts from the GCM projection of the HadCM2 run. This provided monthly values of *Tmax*, *Tmin*, *Precip*, *RHum*, *SRad* for the period 1831 to 2100. The GCM data were then downscaled to the sites and time series of anomalies were used to eliminate GCM internal artefacts and systematic errors. The weather generator C2W (Burger, 1997) was used to disaggregate the monthly climate data to daily. Daily *RHum* and *SRad* were then recalculated.

Tharandt (Germany, GE). Tharandt site is situated in Tharandter Wald near Dresden.

Tharandt site has over 100 year old spruce forest (*Picea abies*) with understory vegetation dominated by *Deschampsia flexuosa*. The forest stand density is 550 stems per ha. The site is situated 20 km South West of Dresden, Germany. Predominant soil type is brown earth (rhyolith). The landscape is not completely flat. The *Tmax*, *Tmin*, *Precip*, *SRad* were available from the Anchor meteorological station in the Tharandt Forest, 50°58'N, 13°34'E at 380 m above sea level from 1959 to 2000.

Loobos (Netherlands, NL). Loobos site has regrowing pine forest stand (*Pinus sylvestris*) with understory vegetation dominated by *Deschampsia flexuosa*. Stem density is 620 stems per ha. This forest was planted on a sand dune in 1917. Landscape is flat. Predominant soil type is sand. Meteorological data as for Brasschaat were calculated using climate data from CRU with climate change impacts from the GCM projection of the HadCM2 run (same method as for Brasschaat).

---

[15] Climatic Research University of East Anglia, Norwich

Aberfeldy (United Kingdom, UK). Griffin forest is a managed sitka spruce (*Picea sitchensis* (Bong.) Carr.) plantation with a stocking density of 2500 stems ha^{-1}. It is situated in gently sloping terrain, has little understory and has a soil stony podsolized brown earth.

The long-term meteorology data set for Aberfeldy was an amalgamation of three different meteorological stations all from the Tayside region of Perthshire, Scotland. Glenshee Lodge, 56°80′N −3°41′E at 335 m, Ashintully Castle, 56°73′N −3°46′E at 341 m, and Kindrogan, 56°75′N −3°55′E at 259 m. Each individual meteorological station had data for *Tmax*, *Tmin*, and *Precip*. A brief analysis was concluded to make assurances that the conglomerate data were not wholly different from the observed data from the EUROFLUX project. This analysis showed that the composite data were marginally cooler (0.72°C y^{-1}), had a lower precipitation (9 cm y^{-1}), a drier atmosphere (1.3 Pa y^{-1}) and received more shortwave radiation (4 W m^{-2}y^{-1}) on average than the observed meteorology from the flux site.

Nitrogen deposition data

Unless mentioned, the nitrogen deposition values (Table 2) for each site came from the project model EMEP[16], and where applicable nitrogen fertilizer was added to this modelled deposition rate of 2 kg N ha^{-1} y^{-1}. The EMEP model is an Eulerian multilayer model with a 50 km horizontal resolution and 20 vertical layers. Within this structure, transport, chemical transformations, and depositions are computed by following an air parcel along a trajectory to a given receptor point. The model is driven by a dedicated weather prediction model and input data of emission inventories submitted officially by individual countries. Deposition values are calculated for both wet and dry nitrogen deposition (Jonson et al., 1998).

Eddy covariance flux data

The method of Eddy Covariance is a non-invasive method of continuous high frequency measurements of carbon dioxide and water exchange simultaneously over several hectares of land (Goulden et al., 1996). However, the methodology is not error free: methodological errors in conjunction with missed fluxes, especially at night, and non random errors from filling data gaps may result in large uncertainties of flux estimates. The gap-filling errors are associated with system failure and a program of data rejection for each site. The flux data from both AMERIFLUX and EUROFLUX used in all analyses were filled with the semi-empirical "Look-Up" method for all sites (Falge et al., 2001b). All errors corresponding to

---

[16] The co-operative Programme for Monitoring and Evaluation of the Long-Range Transmission of Air Pollutants in Europe

this method were calculated using Table 5 in Falge et al. (2001b). The methodological errors were ignored, as their status in the field is still, as yet undecided (Malhi et al., 1999). Daily *RESP* data was calculated using a relationship between night-time temperature and respiration measured by the eddy covariance technique. This was then extrapolated into the daytime (Falge et al., 2001b). *GPP* was calculated as the budget-term of *NEE* and *RESP*.

Model Parameterisation

The site-specific parameterisation of the model was kept at minimum. Only atmospheric CO_2, site physical and general ecophysilology, based on plant functional groups, were specifically parameterised (Table 1, Table 2, and Table 3) for each site simulation. Mainly because of the scale of objectives of the study, and the congruent fact that site specific ecophysiological data are never consistent across the spatial scales involved in regional modelling (Churkina et al., 2003). Extra parameters for phenology, budburst and senescence dates were needed for the simulation of deciduous forests. These were estimated by averaging the first and last days of the carbon uptake period (CUP) for the EUROFLUX and AMERIFLUX data for all years for each deciduous site. The CUP was defined as the period between the first consecutive 5-day period of carbon uptake and the last consecutive 5-day period of carbon uptake.

Model Simulations and Validation

Two types of simulations were conducted in this study: 'spinup' and 'normal' simulations. The 'spinup' simulations were run with the long-term meteorological data to estimate initial state variables for each site at equilibrium. Several test spinup simulations have been performed to determine minimum number of meteorological data to simulate stable carbon pools for given climate (Figure 4). These tests showed that for boreal and temperate sites five years of meteorological data is sufficient.
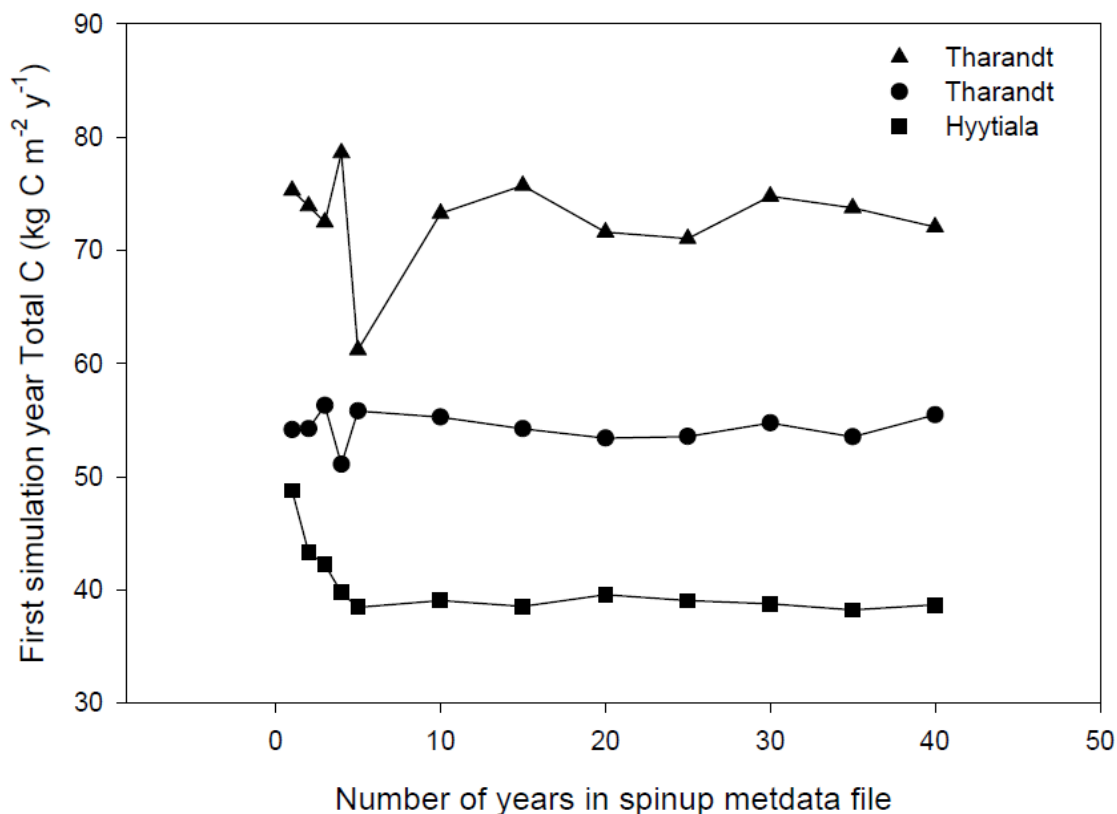
Figure 4. Sensitivity of total carbon pool in spinup simulation to the number of meteorological years for representatives of each biome.

The 'actual growth' methodology from the work of Churkina et al. (2003) was used to initialise state variables for each site 'normal' simulation, where 'spinup' endpoint state variables were reduced by an arbitrary scalar ('young plant', Table 3) to simulate young just planted forests. Then model was run with the number of iterations equal to the published ages of each stand. Finally the model was run for the specific for the same years when eddy covariance data for validations were available for each site. An additional set of model runs were put in practice for deciduous sites:

- one using the internal model for phenology (White et al., 1997)
- one where the phenology for budburst and senescence dates were specified by the user.

All normal simulations were run with the appropriate atmospheric CO_2 concentrations (ppm) and nitrogen depositions (kg N ha^{-1}y^{-1}).

All days on which the data gaps were greater than 25% were removed from both data sets, observed and modelled. This was done to minimise the effect of errors incurred by filling observational data gaps on the analysis, whilst attempting to include days in which useful data still resided (Law et al., 2000). Years in which observational data were missing because of

long term field equipment failure were left out of the all analyses other than those data which where resolved on the daily scale, where erroneous days could be removed.

Results and Discussion

The number of years, climate variability and available validatory data sets gives an opportunity to look at model accuracy across a number of time frames from the daily to the inter annual. It must be remembered through out this section that the data used for *RESP* and *GPP* are only inferred not measured data.

Model phenology

The CUP of a deciduous forest stand is reliant on two things, bud burst having occurred and favourable conditions under which photosynthesis can take place. BIOME-BGC has a sub-routine for deciduous phenology that was tested as part of this study. In the three deciduous sites, modelled CUP was tested against the observed. The start, a proxy for bud burst, the end, senescence, and the number of days, where the individual stands were carbon sinks, were compared (Table 4 and Figure 5).

Table 4. Comparison CUP length, start and end dates of growing season as well as annual NEE with model specified, user specified, and observed phenology.

Site Name	Model Specified Phenology				User Specified Phenology				Site			
	CUP [days]	Start [day]	End [day]	*NEE* [gCm^{-2}y^{-1}]	*CUP* [days]	Start [day]	End [day]	*NEE* [gCm^{-2}y^{-1}]	*CUP* [days]	Start [day]	End [day]	*NEE* [gCm^{-2}y^{-1}]
Soroe	162	104	273	352.1	125	130	257	200.7	132	126	269	63.8
Hesse	195	80	281	426.2	147	127	274	409.5	140	122	278	146.0
Harvard	146	123	287	246.7	121	139	275	269.4	135	141	283	181.3

In all cases the start of the model CUP length was inaccurate. The start dates were on average 22, 42, and 18 days prior to the start dates observed for Soroe, Hesse and Harvard sites respectively. In the worst case scenario the model estimated the start of the CUP to be 53 days (Hesse 1998) and in the best case 2 days (Harvard 1999) prior to the observed. The model predicted the end of the CUP with greater accuracy, overestimating all sites by an average 4 days. The simulation for Hesse proved to be the least accurate at predicting the end of the CUP. In 1998 there was a 22 day overestimation. In 1999 the end date was 20 days earlier than observed. The model overestimated the number of average carbon uptake days by 32, 45, and 11 days for Soroe, Hesse, and Harvard respectively (Table 4). The annual *NEE* was also overestimated for all three sites. Harvard site showed a larger annual average *NEE* with shorter CAP for user specified CUP when compared to model specified CUP. As a way

of reducing these errors for the subsequent analyses, the model was run with user defined starts and ends of the growing season taken from the averages of the observed CUPs. This showed a marked improvement for the start dates of the CUP for all sites but decreased the accuracy of the CUP end dates. Overall the length of CUP periods were on average closer in magnitude to the observed when using user specified phenology approach as opposed to those calculated by the model.
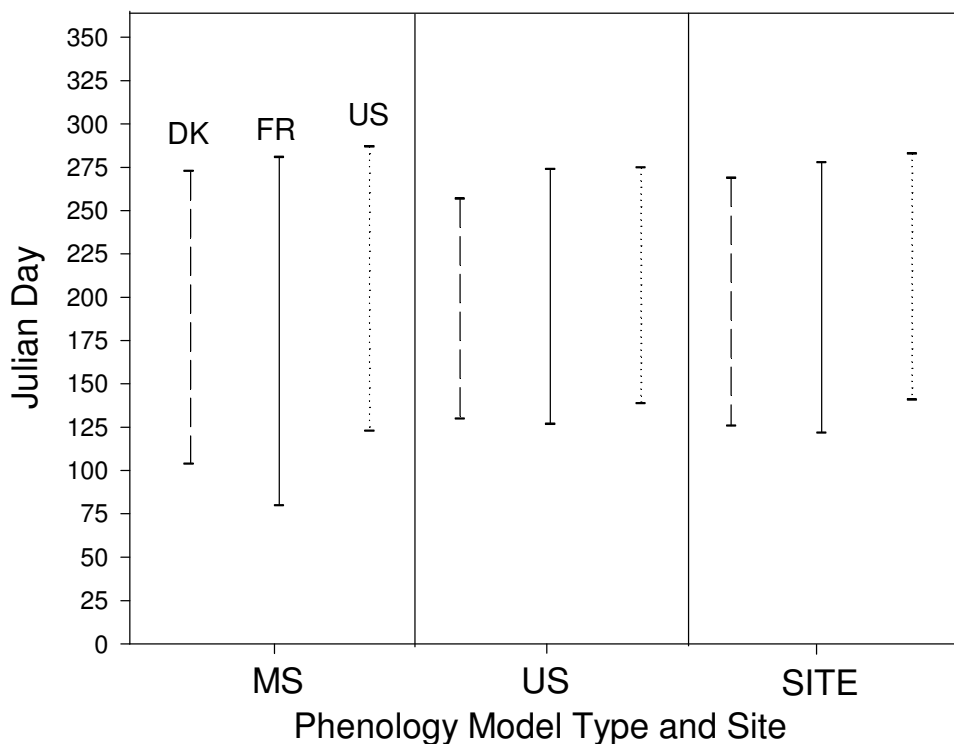

Figure 5. CUP (carbon uptake period) comparisons between Biome-BGC model phenology, user specified phenological and the site carbon uptake period, for the temperate deciduous sites of Soroe, Hesse, and Harvard. The data shown are averages for the sites over the data collection periods.

Overestimations of the CUP length, or inaccuracies in predicting phenological events, can have a large effect on the accuracy of mass exchange in modelled systems (Nizinski and Saugier, 1988)(Table 4), for *NEE* figures. Phenology - bud burst, flowering, seed production and senescence - in all tree species is reliant on the genetics of the species and the abiotic regime, especially temperature and in some cases radiation under which the species resides (Lechowicz, 1984; Murray et al., 1989; Hunter and Lechowicz, 1992; White et al., 1997; Hakkinen et al., 1998; Chuine and Cour, 1999; Chuine, 2000; Chuine et al., 2000). Disregarding the genetics of individual species, one is left with the opportunity to model the

phenological responses. In this case we are interested in budburst, of species to their environment. This creates a trade-off between complexity (Chuine, 2000) and simplification (Hunter and Lechowicz, 1992), generity, especially at the regional and global scales, after all is the holy grail of ecological models (Judson, 1994). The bench mark version of BIOME-BGC dispenses with the radiation term (White et al., 1997), and uses only an exponential of long-term air temperature to calculate a critical sum to budburst. Soil temperature from the first of January is summed to reach this critical value, a spring warming model. 15 days is then subtracted from the onset day to approximate the start of the new growth period, instead of the middle of the new growth period. Hunter and Lechowicz (1992) predicted historical budburst with three types of model:

- spring warming
- winter chilling
- spring warming and photo-thermal.

This study found that a simple spring warming and a winter chilling models are adequate for predicting site level bud-bursts for species with no photoperiodic control. And that across 18 years and 26 species of tree spring warming, sequential chill and parallel chill models were more accurate at predicting budburst than an average day of the year model. However, as this study shows species that are under photoperiodic control, like beech (Lechowicz, 1984), the dominant species for both Soroe and Hesse, cannot be adequately simulated using a simple spring warming model; however it is also stipulated that an annual average model is not sufficient.

Model Validation

Daily Dynamics

Linear regression analysis of daily measured and model *NEE* show relationships (Table 5, all data and all panels in Figure 6) with R^2 values ranging from 0.23 to 0.69 for all the daily data binned and filtered to exclude days with over 25% data gaps. Though not reported in tabular or graphical form in this study the yearly fits ranged from an R^2 of 0.07 for the North Boreas site in 1995 to 0.78 for Tharandt in 1998. The slopes of the regressions vary between 0.43 and 1.11 with intercepts ranging from −1.02 to 0.772.

Table 5. Linear regression results for daily data measured against modelled *NEE* and daily negative (P, carbon release period) and positive (Θ, carbon uptake period) measured against modelled *NEE*[17].

Site Name	N	R^2	b	SE b	a	SE a
Soroe						
All data	1198	0.62	0.333	0.550	0.959	0.022
NEE P 0	721	0.05	-0.641	0.090	0.354	0.060
NEE Θ0	477	0.32	0.899	0.201	0.847	0.057
Hesse						
All data	1176	0.64	0.772	0.089	1.110	0.025
NEE P 0*	700	0.00	-1.290	0.105	-0.020	0.058
NEE Θ0	476	0.30	2.378	0.224	0.826	0.058
Harvard						
All data	1954	0.62	0.351	0.044	0.792	0.014
NEE P 0	1163	0.01	-0.796	0.055	0.113	0.031
NEE Θ0	791	0.29	0.812	0.184	0.735	0.040
North Boreas						
All data	1089	0.23	0.382	0.054	1.030	0.057
NEE P 0*	692	0.01	-0.490	0.746	-0.270	0.108
NEE Θ0	397	0.08	0.862	0.194	0.904	0.153
Hyytiala						
All data	650	0.68	0.055	0.055	1.110	0.030
NEE P 0*	335	0.02	-0.566	0.073	0.258	0.095
NEE Θ0	315	0.47	0.275	0.160	1.056	0.063
Gunnarsholt						
All data	444	0.56	0.204	0.033	0.430	0.018
NEE P 0*	237	0.02	0.044	0.064	0.254	0.100
NEE Θ0	207	0.43	0.452	0.071	0.351	0.028
Brasschaat						
All data	318	0.42	0.001	0.121	1.000	0.660
NEE P 0	182	0.22	-0.037	0.239	1.042	0.460
NEE Θ0	136	0.14	0.505	0.330	0.762	0.161
Tharandt						
All data	418	0.69	-1.020	0.085	1.012	0.033
NEE P 0*	177	0.00	-2.114	0.130	0.140	0.150
NEE Θ0	375	0.45	-1.190	0.157	0.873	0.049
Loobos						
All data	461	0.63	-0.550	0.076	0.950	0.034
NEE P 0	174	0.28	-0.687	0.147	0.887	0.111
NEE Θ0	287	0.41	-0.384	0.168	0.888	0.063
Aberfeldy						
All data	428	0.39	0.470	0.144	0.846	0.052
NEE P 0*	124	0.00	-0.780	0.323	-0.030	0.259
NEE Θ0	304	0.22	0.921	0.251	0.735	0.078

[17] * model is insignificant at the 95% level

The differences seen between the model and the observed data do not however imply that the model is at fault. There are two sources of variance between the measurements and the computations, observation methodological error and footprint evolution, the way in which the footprint of the tower changes and evolves under dynamic climatic conditions (Baldocchi and Wilson, 2001). Harvard is a prime example of the latter in the winter of 1992 and spring of 1993, where anomalous respiration signals were seen. These periods coincided with periods of high winds from the south east extending the footprint to the northwest over a poorly drained bog (Goulden et al., 1996). This effect can be seen as the tail in Figure 6 (US panel), where the model underestimates respiration. Overall, the model is in good agreement with the observed flux data (Figure 6, Table 5) on the daily scale. There are however exceptions, notably the simulations for Boreas and Gunnarsholt.

This analysis was taken further to see if the model could capture seasonality at its most basic level, CUP and carbon release period (CRP), (Table 5). For all sites, excluding Brasschaat, the model was better at capturing the observed variation during the CUP than during the CRP with typical R^2 value between 0.14 and 0.47 for the CUP and 0 and 0.28 for the CRP. During CUP and CRP the slopes suggest an underestimation of *NEE*, though less so for the CUP than the CRP.

With Brasschaat it is not that the variation explained by the model for the CRP is better than any other simulation, the respiration processes are still unrealistic. The difference in comparison with all other sites is that the photosynthetic processes at the start of the CUP are not modelled well in 1998 and though not shown here, worse for 1997. The pattern seen in the *GPP* and consequently the *NEE*, a severe slump at the beginning of the CUP is present at no other site. The meteorology data for the simulations was checked to see if there is a climatic explanation for the reduced productivity, none could be found. However, it was found that there were no reliable eddy covariance measurements for the periods 7th April to 26th June 1997 and from 12th May to 15th June 1998 (Carrara A., personal communication), giving rise to the discrepancies for this site. In conjunction with this knowledge the Brasschaat site was removed from subsequent annual analyses.

From this analysis of CUP and CRP one could assume that the model has a better predictive capacity for processes related to photosynthesis than respiration. This however may not be the case, it maybe be that both respiration and photosynthesis are being overestimated leaving an *NEE* signal that to all intents and purposes looks accurate with respect to the observed during the CUP.
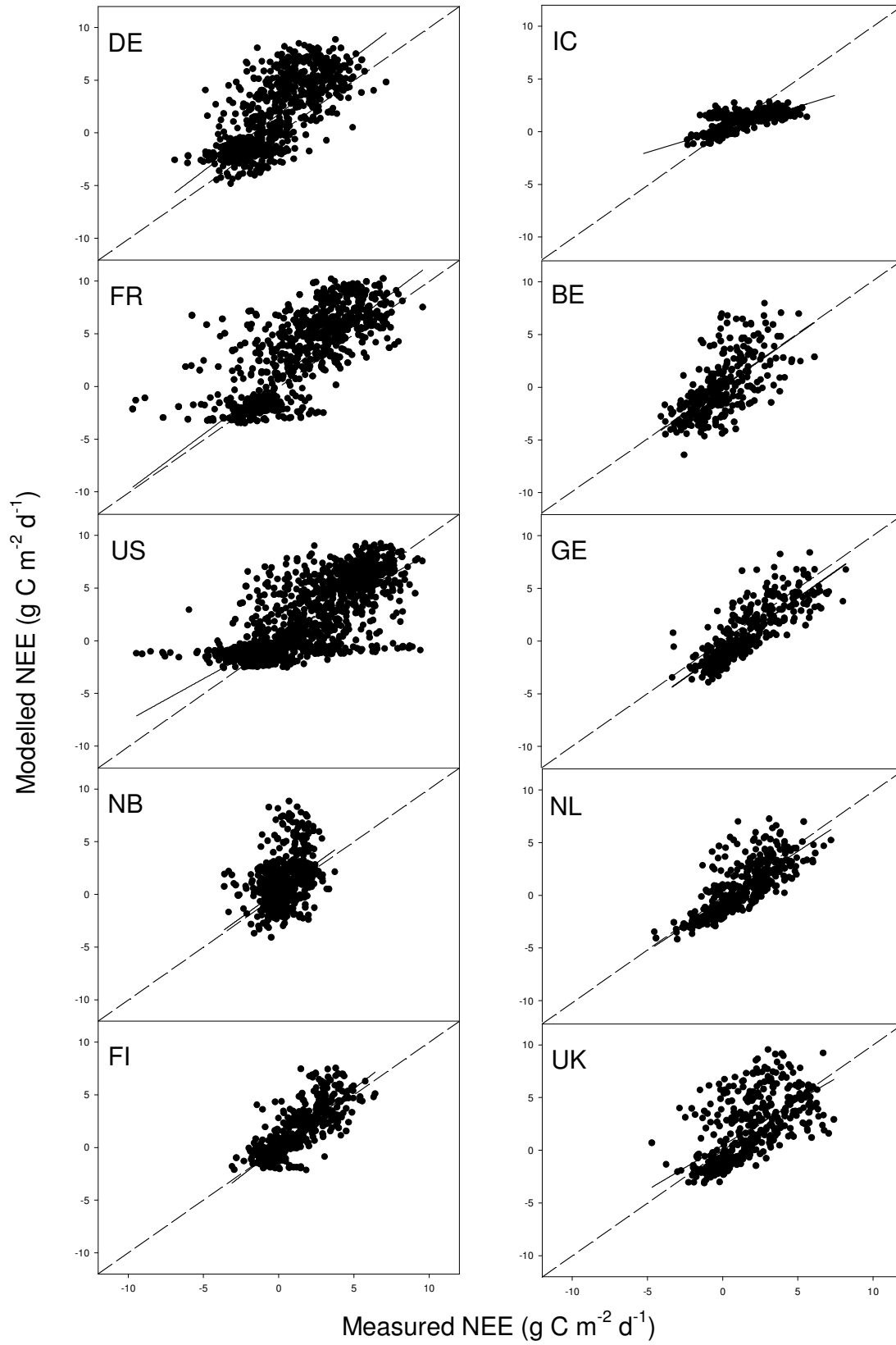
Figure 6. Linear regressions between modelled and observed flux data and the 1:1 regression line for 10 sites.

The response of the modelled *RESP* to temperature is markedly different to that inferred from the observed *NEE* for both boreal and temperate coniferous (Figure 7). It must be noted that the rate of carbon efflux from the modelled system is not solely dependent on temperature. Water and nitrogen availability are also limiting factors but will not be discussed here. All sites were considered not to be drought-limited and most had adequate atmospheric nitrogen deposition. The difference in temperate deciduous biomes is less clear. It was assumed that the relationships were exponential (Table 6), though the relationship for temperate deciduous biomes could be expressed in a piece-wise manner. The data was then linearised buy using the natural logarithm of *RESP*, for both the observed and the modelled data. Statistically both the slopes and intercept of all biomes were different. This was shown by using dummy variable multi-linear regressions (Table 6).

Table 6. The model estimates of the exponential[18], and linearised fits of *RESP* and temperature for temperate deciduous (TD), boreal coniferous (BC), and temperate coniferous (TC) biomes.

Biome type	N of sam ples	Exponential estimates				Linear estimates			Dummy Variable Analysis	
		R^2	C	b0	b1	R^2	b	a	$b_{model} \neq b_{site}$	$a_{model} \neq a_{site}$
TD model	3619	0.68	−69.6	4.3	0.0023	0.49	0.194	0.064	p = 0.00	p = 0.00
TD site	3619	0.74	−3.49	1.5	0.028	0.59	0.1	0.067		
BC model	519	0.87	−1.53	0.93	0.045	0.75	−0.161	0.085	p = 0.00	p = 0.00
BC site	519	0.95	−0.38	0.72	0.056	0.89	0.51	0.061		
TC model	1215	0.76	−1.56	5.06	0.0013	0.63	0.32	0.071	p = 0.00	p = 0.00
TC site	1215	0.90	−0.68	1.16	0.0539	0.78	0.93	0.061		

For coniferous biomes the slopes for the model estimates were lower than for the sites; the modelled data intercepts were greater. And visa versa for deciduous biomes, in all respects the difference between the slopes and the intercepts is negligible, in the order of 0.09 for the intercept and 0.003 for the slope and the statistical viability is questionable because of the large N=3616. R^2 values for ranged from 0.49 to 0.89. For coniferous biomes the analysis shows that at lower temperatures the model overestimates respiration yet at higher temperatures the model estimates for *RESP* and the sites are closer to equality. Thus, the *RESP* is overestimated during the low temperatures of winter. *GPP* was not included in this analysis with temperature because the processes involved, especially assimilation rate, though

---

[18]The exponential has the form $y = C + e^{(b0+b1x)}$ this model was fitted using the loss function of least squares in STATISTICA. a is slope, b is intercept.

effected by temperature is driven more directly by photosynthetic photon flux density (PPFD) (Jarvis *et al* 1997).
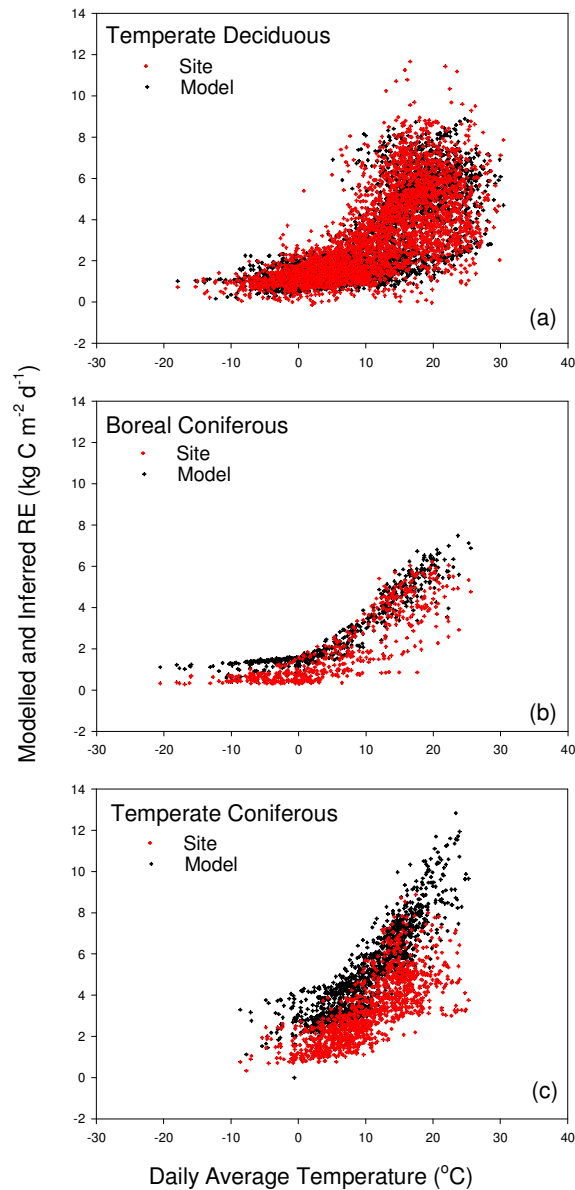

Figure 7. Response of the site ecosystem and the modelled ecosystem respiration to temperature. (a) Temperate deciduous, daily data for Soroe, Hesse and Harvard. (b) Boreal coniferous, daily data from Hyytiala. (c) Temperate coniferous, daily data from Brasschaat, Tharandt, Loobos and Aberfeldy. The responses of *RESP* to temperature modelled (red) and inferred from the observed *NEE* (black) are in good agreement for the temperate deciduous biome (a). For both coniferous - boreal (b) and temperate (c) - the modelled *RESP* is strongly overestimated.

Seasonal Dynamics

The time series of representatives from each biome type (Hyytiala 1998, Hesse 1999, and Loobos 1997) were used to comment on the accuracy of the model at the intra-annual and seasonal level (Figure 8). For all three sites, the model followed the seasonal trend with some level of accuracy. Distinct patterns were also followed - the end of the growing season out-gassing in both temperate deciduous and boreal coniferous biomes was well met. The order of magnitude of the *NEE* between the estimated and observed during the CUP in all cases was in good agreement. There was a startling deviation between the two data sets and that is the overestimation of the respiration during the CRP.
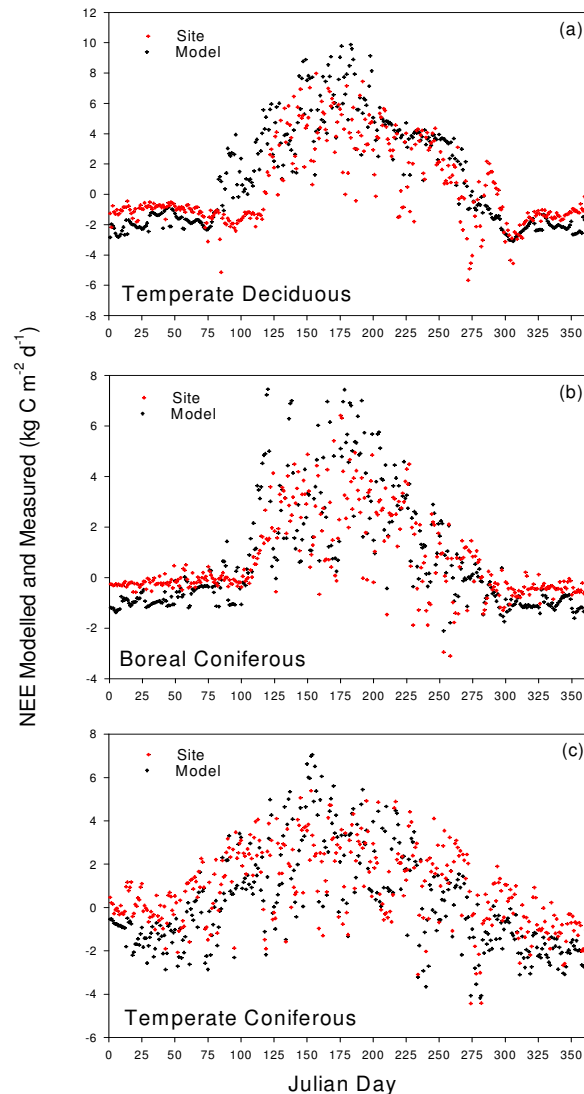

Figure 8. Seasonal variation, comparison between daily site measurements and model estimates for. (a) Temperate deciduous, Hesse, 1999, (b) Boreal coniferous, Hyytiala, 1998 and (c) Temperate coniferous, Loobos, 1997.

Annual Sums

The annual sums for *GPP*, *RESP*, and *NEE* are shown in Figure 9 (a, b and c), where each biome type can be seen independently of one another. Overall the relationship was best for *GPP*, then *NEE*, and finally *RESP*, with the slopes of 1.6, 0.55, and 1.25 respectively. The slopes for *GPP* and *RESP* suggest overestimations by the model at all sites with high productivity and biological activity and underestimations at sites with poor productivity. The slope for *NEE* suggests the opposite.
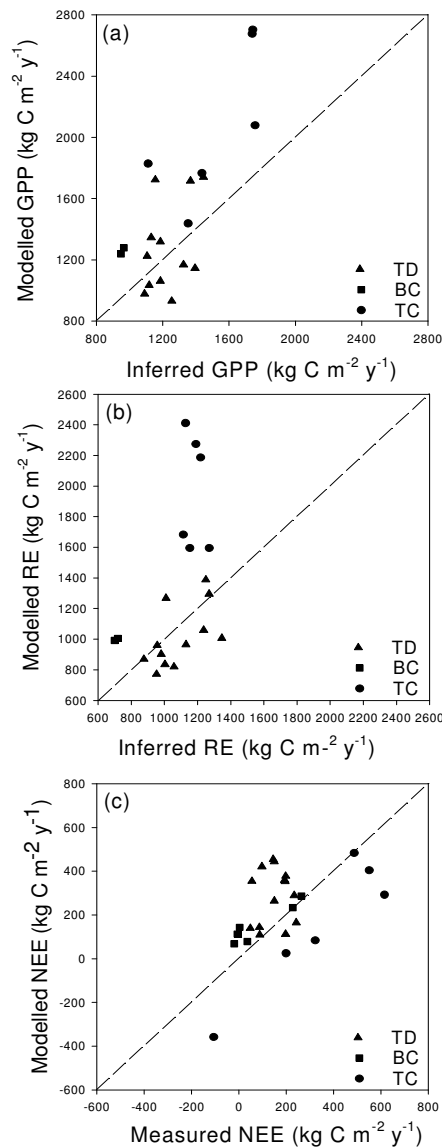

Figure 9. Modelled vs. observed (inferred from observations) fluxes of *GPP* (a), *RESP* (b), and *NEE* (c) for temperate deciduous (TD), boreal coniferous (BC), and temperate coniferous (TC) biomes.

56% of the variation in *GPP* was explained by the model, suggesting as did the CUP and CRP daily fits that the photosynthetic processes are realised with greater accuracy by model than are the respiratory processes. While modelled *NEE* proved less predictive in nature with $R^2 = 0.23$. BIOME-BGC was least accurate at predicting respiration, $R^2 = 0.15$. The overestimation of *GPP* was the greatest for coniferous biomes, with model estimates for temperate coniferous biomes being less accurate that those for boreal coniferous biomes. *GPP* for temperate deciduous biome were not systematically over- or under-estimated by the model but spread above and below the 1:1 line. The trends for *RESP* showed similar patterns to those for *GPP*. *NEE* is the difference of *GPP* and *RESP* and as such shows a mixed signal, of those biomes where either *RESP* or *GPP* are the dominant processes. Those coniferous biome sites which alight on the 1:1 line do so purely as a result of both a *GPP* and *RESP* overestimation, as was alluded to earlier in this section. Deciduous biomes on the other hand fall around the 1:1 line as a result of fairly accurate predictions of both *GPP* and *RESP*. All sites in the study can be seen to be both measured and modelled sinks of atmospheric CO_2, except Brasschaat, the reasons which were discussed earlier.
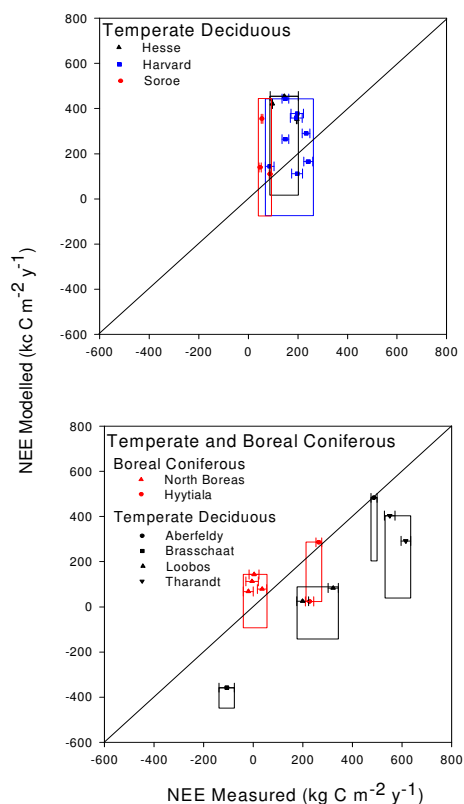

Figure 10. Relationship between annual modelled and measured NEE and its uncertainty for different forest biomes. Uncertainty for measured NEE is calculated from site error estimates based on gap filling technique. Model uncertainty estimates are

based on parameter simulation treatment: (a) Temperate deciduous, model estimates are calculated from two different initial state variable estimates and phenological model. (b) Boreal and temperate coniferous, model estimates based solely on the two different initial state variable conditions.

Both the model and the site measures are subject to error, either from gap filling in respect to the site observations or from an initial parameterisation in the model. Figure 12 shows what we have termed as the error/estimate space. In Figure 10a it can be seen that for all biomes the effect of interannual climate variability is undetectable, in that for all biomes the site errors are overlapping. It can also be pointed out that even though on different continents, the *NEE*'s for Hesse and Harvard a not different from one another. For the coniferous biomes (Figure 10b), only Boreas has an undetectable effect of interannual climatic variability, all other sites show distinct differences between simulation years. One can also see from the nature of the spread of the error spaces that each site can be considered as different from one another with respect to *NEE*, unlike the deciduous biomes.

Our results suggest that the model has a propensity to overestimate the *RESP* of modelled biomes. This has been seen in other of other biogeochemical models when validated using CO_2 flux data, CANOAK (Baldocchi and Wilson, 2001), Forest-BGC (Cienciala et al., 1998a) and BIOME-BGC (Thornton et al., 2002; Churkina et al., 2003) and CANPOND (Law et al., 2000). These errors in *RESP* appear to be more consistent in coniferous biomes. As can be seen in Figure 1, the biomes on the European continent are not so different from one another to expect that the accuracy of the deciduous sites stem from climatic differences. This then presents the idea that the increased model accuracy for simulating deciduous biomes is in response to some initial stock sizes, such as soil carbon, stem carbon and leaf carbon.

Only two sites have a long enough data set, Harvard and North Boreas. Figure 5, to corroborate the model at the interannual level. As would be expected from the annual fits the figures for model annual *NEE* are not in good agreement with those observed, though they are of the correct order of magnitude. The model does not however pick up the interannual trends seen in the flux data.

Problematic sites

North Boreas

Of all the simulations, simulated carbon fluxes for the North Boreas site has the least significance in relation to the observed ecosystem fluxes. BIOME-BGC can be seen to overestimate *NEE*, Figure 11b. The one physical trait of this site that is present in none other

is the presence of permafrost. The reason for the chronic inaccuracy of the model for this site can be linked to the inability of the model to properly represent soil temperatures profiles in a cryogenic soil. In Figure 11 the site soil temperature profile and *NEE* are plotted with model soil temperature (no profile since soil temperature is assumed to be constant through the rooting zone) and *NEE*. The model can be seen to simulate the upper 5cm of the site soil profile well, this being the zone which is most coupled with the atmosphere. Because there is only one soil pool there can be only one soil temperature, this removes the possibility of the model capturing soil profile dynamics. Meaning that while the model vegetation has the whole of rooting depth free (available soil water) for uptake to take place from day 130, the site has only the top 5cm available from day 136. With this limited depth of unfrozen soil at the site - as common sense would predict, because water is limited (frozen) - stomatal conductance will be minimal. In turn reducing the ability of the site vegetation to maximise the light available for photosynthesis. This is the reason for the discrepancy between the model and site *NEE* early in the growing season. Under this same logic one would expect the site *NEE* to increase as the permafrost level drops throughout the growing season as more soil resources are made available. This is not the case. A similar pattern of site seasonal *NEE* for 1995 can be seen in (Rayment and Jarvis, 1997) and can be attributed to the difference in phase between the photosynthesis and respiration during the growing season. The simple logic that the *NEE* increases with increases availability of unfrozen soil does not hold because while photosynthetic rate and soil respiration are increasing in response to increasing temperature. Branch bag measurements show photosynthesis occurs from day 100 to day 300 with peak the photosynthetic period being approximately between days 150 and 235, while soil respiration processes peak between days 190 and 250. The resulting pattern of *NEE* shows peak uptake between days 140 and 190, from this period approximately to day 210 of the CUP the *NEE* reduces and then fluctuates around equilibrium till the end of the growing season (Rayment and Jarvis, 1997). This is the same pattern as seen at the Boreas site in 1995 as well as all other years in this study. The model on the other hand assumes that the whole soil depth becomes defrosted, therefore water is freely available earlier than observed, when in fact only the top 5cm is, allowing photosynthesis to occur at a rate constrained only by the atmospheric climatic conditions. The rest of the model time series incorporates the same downward trend in *NEE* towards the end of the CUP.
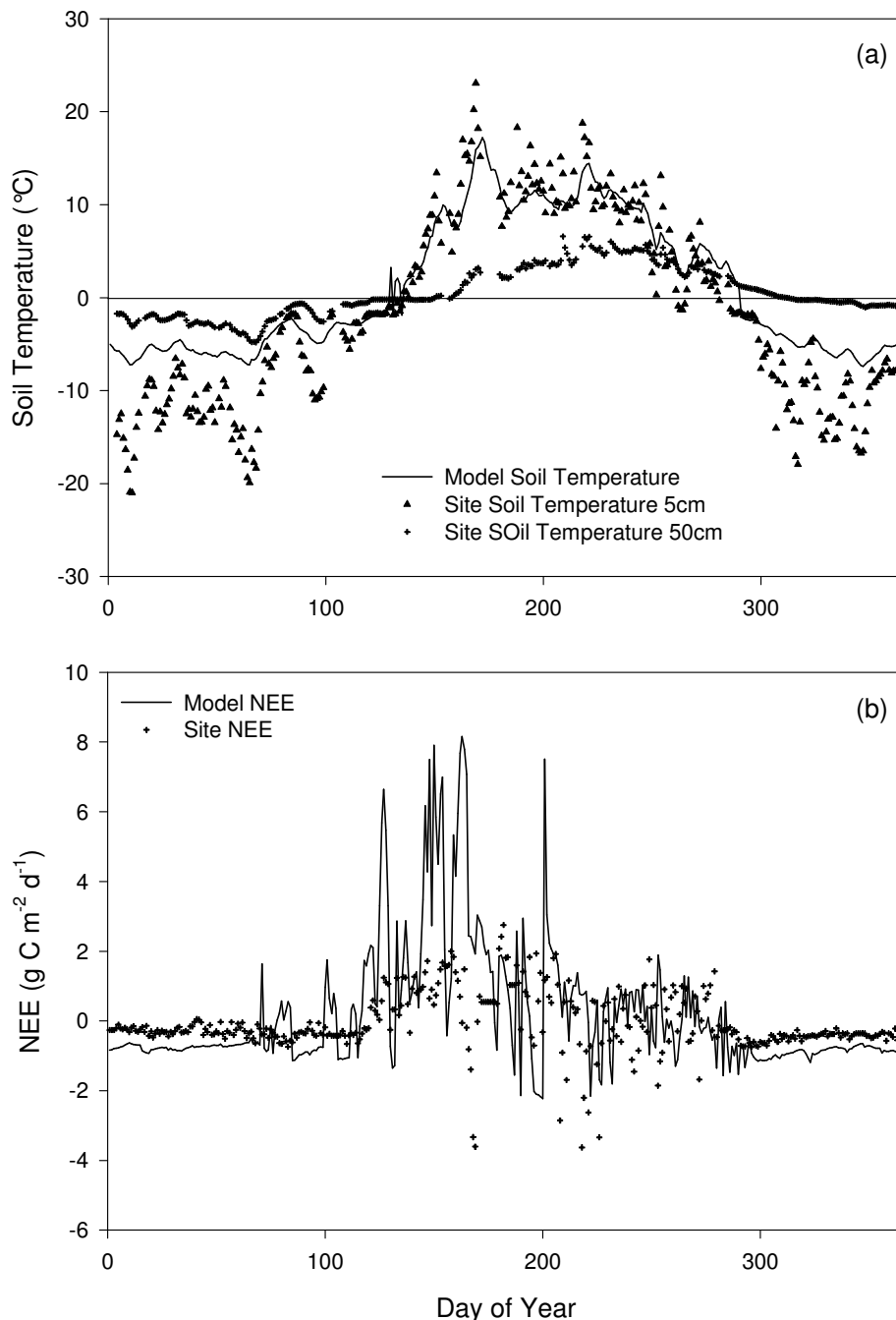
Figure 11. Modelled and measured soil temperatures (a) and NEE (b) for North Boreas site. (a) Soil profile measures from Boreas at 5 and 50cm and modelled soil temperature (°C) for 1995. (b) Time series for modelled and measured NEE (gC m^{-2}yr^{-1}). Effect of permafrost on NEE is not captured by the model.

New problem, PHS and TRANS appear to be occurring during periods where soil temperature is below freezing – BOREAS – this is counterintuitive and should cause cavatiation in the tree. There are 6 distinct periods when soil T is less than 0 where carbon uptake occurs, all on days where mean air temperature is greater than 0. This should not happen since g should be reduced to nearly 0, to prevent cavitation. This is because there is no realisation of the effect of sub-zero soil temperatures on soil water availability and

consequently stomatal conductance (g) in BIOME-BGC. This is not representative of the true processes, since g in forest stands with frozen soils should be reduced to nearly zero as prevention to cavitation. Some data from 1994 suggest that this is the case, with typical daylight average *g* of 0.0003 m s^{-1} -some 3.8% of the global g_{max} reported for coniferous forests (Waring and Running, 1998) - on year day 103, a bright clear day with snow and ice cover (Zimmerman, R., personal Comm.). This effect is not seen in any of the other simulations because of the lack of permafrost, i.e. if the soil is frozen it is only the top few cm and so water is still available to the plant at lower depths. The observed *NEE* does not show this inconsistency, the first days of carbon uptake are seen after the thawing of at least the top 5 cm of soil.

Even after first thawing of the soil it takes time for the plant to biogeochemically reorganise for photosynthesis. Tree would still be in its dormant phase.

Gunnarsholt

The major problem with the Gunnarsholt simulations is the lack of long-term coherent flux data from measurements. This is why the site is missing from the majority of the analyses. The model at the daily level also calculated the *NEE* to be lower than that measured at the flux station. In assessing this site one must remember the management that has occurred at the site and that the treatment of this in the model may not be totally accurate. This was the only occurrence in the study where the state variables were modified to try to simulate the implication of forest management and not just stand age.

Conclusions

Phenology

For simulations at the regional scale the inability of the model to predict CUPs for species under photoperidic control is a problem that needs to be rectified. This is of great importance in accurately estimating the *NEE* over large areas.

Respiration

The representation of the relationship between *RESP* and temperature exceeds those observed seen at low temperatures but is in good agreement with the observed relationships at higher temperatures, suggesting that the functional relationship between the two needs to be adjusted.

Boreal sites

Work needs to be done on the model with respect to the inclusion of a number of soil layers in the vertical to resolve the profile dynamics seen in boreal soils. The effect of frozen soils must also be used as a constraint on g so that in favourable atmospheric conditions the model does not calculate.

Parameter estimation for the terrestrial ecosystem model BIOME-BGC using eddy-covariance flux measurements

By Kristina Trusilova and Galina Churkina

Overview of Previous Studies

It has been suggested that models can be calibrated and estimates of regional (and global) carbon fluxes could be improved using a combination of various types of observations (Wang et al., 2001). To produce the best estimate of the carbon budget we need to make use of all available constraints implied by the different data sources, as well as the physiological and ecological constraints embodied in the models. Raupach *et al.* (2005) reviewed model-data synthesis tools targeted to estimate various components of terrestrial carbon cycle. They provided an insightful theoretical discussion of the Bayesian approach in comparison to other methods available for model-data synthesis. Van Oijen *et al.* (2005) utilised Bayesian methodology to calibrate the parameters of a process-based forest model BASFOR using parameter values taken from literature and measurements of 13 output variables taken at a Norway spruce site. They found that constraining tree height and NPP already reduced posterior uncertainty significantly. Having data of greater precision, or longer time series, gave further improvement. Wang *et al.* (2001) used the nonlinear inversion approach to estimate parameters of the surface-exchange model CSIRO Biosphere Model (CBM) constraining model outputs by hourly fluxes of CO_2, latent heat, sensible heat, and soil heat measured during a period of three weeks in 1995 at six different forest sites in SE Australia. They found that only four parameters of the CBM model could be independently constrained from the observations for all sites. Measurements of the ground heat flux provided little information about any of the model parameters. Braswell *et al.* (2005) used Bayesian parameter estimation technique to constrain parameters of a simplified Photosynthesis and EvapoTranspiration model (SIPNET) with hourly net CO_2 flux series in the time period 1992-2001 at one forest site. The purpose of this study was not to calibrate the model, but to understand how much information about controls on ecosystem processes can be derived directly from *NEP* observations. The SIPNET initial carbon pool values, physiological, photosynthesis, respiration and moisture parameters were highly constrained by the flux data at daily and seasonal timescales. Most of the abovementioned studies aimed at a better parameterisation of the models or understanding of ecosystem processes in the models using

measurements taken at one site. The only application of the model-data synthesis tools at multiple sites (Wang et al., 2001) used very short time series of data (three weeks).

Objectives

In this technical report we use measurements of carbon fluxes taken at six forest sites in conjunction with previously available information on parameters of the ecosystem process model BIOME-BGC (Running and Hunt, 1993) in order to improve modelled estimations of carbon fluxes. Since both types of information are uncertain, Bayesian probabilistic fitting method (Mosegaard and Tarantola, 1995) was chosen in our study. We investigate which observations or which combinations of them better constrain the model parameters and which model parameters are the most critical for the improvement of carbon flux estimates. Finally we test if our approach is suitable for development of a general forest parameterisation and discuss uncertainties associated with application of this parameterisation in simulations of regional or continental carbon budgets.

Model Parameterisation

The original set of ecophysiological parameters of the model includes 47 constants (Table 1). Since only one-year observations were available for this study, only 14 parameters which characterise fast ecosystem processes were included in the optimisation (Table 7). Parameters describing slow ecosystem processes, like carbon allocation to different ecosystem pools, plant mortality, etc. were excluded from the optimisation because the one-year observations do not provide sufficient information to constrain these parameters. Into the optimisation scheme we also added four parameters which describe decomposition processes in the soil (Table 7).

Table 7. BIOME-BGC model parameters chosen for optimisation and their units. All parameters except E_0, T_0, T_{ref}, and *Minpsi* are the EcoPhysiological Constants (EPC) which characterise a particular vegetation type within the model; the parameters E_0, T_0, T_{ref}, *Minpsi* characterise soil decomposition processes.

Parameter	Description	Units
CNl	C:N ratio of leaves	kgC/kgN
CNll	C:N ratio of leaf litter, after retranslocation	kgC/kgN
CNfr	C:N ratio of fine roots	kgC/kgN
CNlw	C:N ratio of live wood	kgC/kgN
CNdw	C:N ratio of dead wood	kgC/kgN
SLA	Canopy average specific leaf area	m^2/kgC
FrNRub	Fraction of leaf nitrogen in Rubisco	DIM
MaxSC	Maximum stomatal conductance	m/s
Ccond	Cuticular conductance	m/s

BLcond	Boundary layer conductance	m/s
LWPs	Leaf water potential: start of conductance reduction	MPa
LWPe	Leaf water potential: complete conductance reduction	MPa
VPDs	Vapour pressure deficit: start of conductance reduction	Pa
VPDe	Vapour pressure deficit: complete conductance reduction	Pa
E_0	Activation-energy-type parameter of decomposition (Lloyd and Taylor 1994) – energy required to bring all molecules in a chemical reaction into the reactive state	$°C^{-1}$
T_0	Soil temperature when all decomposition processes stop	°C
T_{ref}	Reference soil temperature in the equation 11 in Lloyd and Taylor (1994) for calculation the base decomposition rates	°C
Minpsi	The minimum values for water potential limit for calculation of the soil water content	MPa

The BIOME-BGC model was initialised with two sets of ecophysiological parameters for three deciduous broadleaf and three evergreen needleleaf forests (Table 8) and with six site-specific sets of parameters such as latitude, elevation over the sea level, atmospheric nitrogen deposition, as well as soil texture and depth (Table 9). This parameterisation reflects two important model assumptions:

1) coniferous and broadleaf forest stands have the same physiological structure,

2) the difference in forest functioning within coniferous or broadleaf type stems is mostly governed by site-specific environmental conditions.

Table 8. Initial values and ranges of model parameters for deciduous broadleaf and evergreen needleleaf forests. The parameter ranges are as in (White et al., 2000).

Parameter	Deciduous broadleaf forest		Evergreen needleleaf forest	
	Initial Guess	Range	Initial Guess	Range
CNl	24.0	16.3 - 35.7	42.0	22.8 - 70.0
CNll	49.0	16.3 - 114.0	93.0	49.0 - 143.0
CNfr	42.0	25.0 - 75.8	42.0	27.6 - 200.0
CNlw	50.0	25.0 - 76.0	50.0	28.0 - 200.0
CNdw	442.0	421.0 - 819.0	729.0	212.0 - 1400.0
SLA	30.0	16.3 - 66.7	12.0	2.0 - 21.0
FrNRub	0.08	0.075 - 0.085	0.04	0.035 - 0.045
MaxSC	0.005	0.004 - 0.006	0.003	0.002 - 0.004
Ccond	$1.0 \cdot 10^{-5}$	$0.5 - 1.5 \cdot 10^{-5}$	$1.0 \cdot 10^{-5}$	$0.5 - 1.5 \cdot 10^{-5}$
BLcond	0.010	0.005 - 0.015	0.08	0.075 - 0.085
LWPs	−0.6	−0.5 - −0.2	−0.6	−1.0 - −0.2
LWPe	−2.3	−3.5 - −1.3	−2.3	−5.0 - −1.4
VPDs	930.0	500.0 - 2000.0	930.0	500.0 - 1000.0
VPDe	4100.0	2300 - 4700.0	4100.0	2000.0 - 6000.0
E_0	35.4	25.0 - 45.0	35.4	25.0 - 45.0
T_0	−46.0	−50.0 - −42.0	−46.0	−50.0 - −42.0
T_{ref}	25.0	15.0 - 30.0	25.0	15.0 - 30.0
Minpsi	−10.0	−15.0 - −5.0	−10.0	−15.0 - −5.0

The initial values for the ecophysiological parameters (Table 8) for both deciduous broadleaf and evergreen needleleaf forests and their ranges were set as in the work of White et al. (2000) Initial values of the decomposition parameters where set according to Lloyd and Taylor (1994).

Table 9. Site and plant functional characteristics of the study sites. For deciduous forests the beginning and the end of the growing season were set, for evergreen forests - automatically defined by the model.

Site code	Site name	Lat	Lon	forest age in 2001 [year]	Growing season [day]	Elevation [m]	Soil Type
Deciduous broadleaf forest stands							
HA	Hainich	51°05' N	10°28' E	250	125 – 280	445	cambisol
HE	Hesse	48°40' N	07°05' E	36	124 – 295	300	luvisol
SO	Soroe	55°29' N	11°38' E	81	144 – 295	40	cambisol
Evergreen needleleaf forest stands							
HY	Hyytiala	61°51' N	24°17' E	40	-	170	till
LO	Loobos	52°10' N	05°45' E	91	-	25	sand
TH	Tharandt	50°58' N	13°34' E	114	-	380	rhyolith

Model Simulations

Carbon and nitrogen state variables of the BIOME-BGC model represent amounts of carbon and nitrogen stored in simulated plant and soil pools. Unless values for the initialisation of the model's state variables are available from measurements, model simulations are required for their initialisation (spin-up run). In the spin-up run, the model is run to a steady state to obtain the size of the ecosystem's carbon and nitrogen pools under the assumption of ecosystem being in equilibrium with the long-term climate. The spin-up run requires long term climatic variables, which would represent long-term interannual climate variability necessary to generate plausible values for carbon and nitrogen pools. Although most ecosystem are far from equilibrium because of human and natural disturbances, the spin-up run is often used in ecosystem modelling because measurements of all state variables are rarely available and land use or management history becomes harder to obtain as we move from local to regional scale simulations.

In this study, spin-up runs for all six sites were performed with pre-industrial values of atmospheric carbon dioxide concentration (287.2 ppm) and atmospheric nitrogen deposition two kg ha^{-1} yr^{-1} (Holland et al., 1999). The daily climate data used for spin-up runs were from 50 to 80 year long on average (Table 10).

Table 10. Meteorological and nitrogen deposition data used in the BIOME-BGC model simulations for selected sites. The short-wave radiation measurements (TACOS database) were used to correct the radiation calculated by the MTCLIM. The nitrogen deposition data of the Hainich site were used for all high-nitrogen-deposition study sites (High N dep.); for the Hyytiala site the site specific data were used (Low N dep.).

Site code	Available meteorological data [year]	Mean T [C°]	Precip. [mm/year]	Shortwave radiation measurement data [year]	Industrial nitrogen deposition
HA	1951-2001	7.0	750	2000-2001	High
HE	1950-2001	9.2	885	1997-2001	High
SO	1916-2001	8.1	510	1998-2001	High
HY	1959-2001	3.5	640	1997-2001	Low
LO	1941-2001	9.8	786	1997-2001	High
TH	1952-2001	7.5	820	1997-2001	High

Effects of ongoing environmental changes on forests in Europe were reflected in the subsequent "normal" run. Stand growth was simulated with continuously increasing atmospheric carbon dioxide concentrations and nitrogen deposition in the 20th century. The CO_2 concentration in the atmosphere has increased from the pre-industrial value of 287.2 ppm at the end of the nineteenth century to the average value of 371 ppm measured in 2001. Atmospheric nitrogen deposition was assumed to be at a pre-industrial level of 2 kg/ha before 1959 and continuously increasing afterwards. For the sites with high-nitrogen deposition (Hainich, Hesse, Soroe, Loobos and Tharandt) the same nitrogen deposition time series were used as in the work of Churkina *et al.* (2003). For the Hyytiala site, the nitrogen deposition rates were considerably lower than at the other sites; these data were taken from the work of Kulmala *et al.* (1998b).

The climate data required to drive the BIOME-BGC model were obtained from meteorological stations located at or near the sites of carbon flux measurements. Since daily average shortwave radiation and vapour pressure deficit were not available from meteorological stations for most years, these climatic variables were obtained using the Mountain Climate Simulator MTCLIM (Thornton et al., 2000). MTCLIM is a climate simulator, which estimates daily average shortwave radiation and vapour pressure deficit from maximum and minimum daily temperatures and precipitation. Measured shortwave radiation

data for 2001 were available from the TACOS database[19] and were used here for simulations of carbon fluxes in that year for all sites.

Observational Data

Six forest stands were selected to represent natural vegetation in Europe. The dominant vegetation at each site was either deciduous broadleaf or evergreen needleleaf forests. The sites are located in different climate zones, at different elevations and are characterised by different forest ages and soil types (Table 9). For testing the model performance with the optimised parameter set we chose two additional sites: a deciduous broadleaf forest at Le Bray (France) and an evergreen needleleaf forest at Vielsalm (Belgium). The measurements taken at these sites were not included in the parameter optimisation process and, thus, were used as an independent data for validation of the model performance with the optimised parameter set.

The net carbon fluxes were measured using the eddy covariance method (Aubinet et al., 2000). Half-hourly night-time *NEP* fluxes were filtered according to a u-star threshold criterion (Reichstein et al., 2002), gap-filled (Falge et al., 2001a; Falge et al., 2001b) and separated into two main components: *GPP* and *RESP* (Falge et al., 2001a; Falge et al., 2001b; Reichstein et al., 2005). The gap-filling algorithm is a combination and enhancement of methods offered by Falge et al. (2001b). The algorithm searches for similar meteorological conditions, within the shortest possible time window and fills the missing value with the average flux during those conditions. That way the gap-filling algorithm exploits both the correlations between meteorological drivers and fluxes as well as the temporal autocorrelation of the fluxes. The flux-partitioning algorithm searches for a temperature response in short-term data. The ecosystem respiration, *RESP*, was calculated based on an extrapolation of night-time CO_2 flux measurement to daytime using a non-linear regression with temperature and soil moisture. *GPP* was calculated as difference between *NEP* and *RESP*.

Measured values of maximum projected leaf area index were obtained from the CARBOEUROFLUX[20] and the TACOS projects databases.

Uncertainties

The uncertainty estimation is one of the crucial points in every study where measured and modelled data are used. The accuracy of the model parameters depends on the variability of the parameters within the 'footprint' area of the measurements. This variability may result from heterogeneity of soil conditions, plant species, and measurement errors. The question

---

[19] www.bgc-jena.mpg.de/public/carboeur/projects/tacos.htm

[20] http://gaia.agraria.unitus.it/database/carboeuropeip/

about uncertainties rose relatively recently when model calibration tasks required more and more precision from measured data and, hence, their reliability. Uncertainties in eddy covariance measurements arise from several sources. Statistical, random errors are generally small (<5%) due to the large number of measurements taken (Goulden et al., 1996). Systematic instrumental errors may also be small (up to 5%-10%), if instruments are carefully cross-calibrated and maintained (Baldocchi and Bowling, 2003). The largest uncertainty (10%-30%) in eddy covariance measurements is related to low turbulence conditions during night-time and depends on the local topography and stand characteristics (Goulden et al., 1996; Knohl et al., 2003).

At the moment, there is no standard method to estimate the uncertainty of measurements, but one can estimate the uncertainty of the model. To do that, we suggest including a priori information about model parameters and their uncertainties into the optimisation. This estimation of parameter uncertainties is expected to be reduced by the optimisation procedure.

Nonlinear inversion

Measured carbon fluxes and maximum projected *LAI* were used to improve initial estimations of the model parameters $\mathbf{m_{init}}$. Sampling different parameter values $\mathbf{m}$ iteratively we maximise the target function (*TF*) which defines the match between the model output and the observational data:

$$TF(\mathbf{m}) = p(\mathbf{m}) \cdot L(\mathbf{m}), \qquad \qquad \textbf{Equation 1}$$

where

p($\mathbf{m}$*)* - probability density function that represents a priori knowledge on parameter values,

L($\mathbf{m}$*)* - likelihood function, a measure of the degree of fit between model output and observations.

Due to the complex structure of the model the relationship between the input parameters and the output is highly nonlinear and, therefore, the maximisation of *TF* can not be performed analytically. We use the Metropolis algorithm (Bayesian analysis and the Markov Chain Monte Carlo sampling procedure) to search the multidimensional parameter space and to sample parameter posterior distributions (Tarantola, 1987). The Metropolis algorithm belongs to a class of global search methods based on random sampling of parameter posterior distributions and quantifies parameter uncertainties as well as model output uncertainties. We did not use other optimisation methods like Downhill Simplex method or Conjugate Gradient method in multi-dimensions because they search for a local minimum and do not sample posterior distributions of parameters – an important source of information about the optimised

parameters. An accurate description of the Metropolis algorithm can be found in the appendix to the paper of Braswell *et al.* (2005).

The second term in the Equation 1 is the likelihood function *L(***m***)* which quantifies the degree of fit between the model output and the observations. The likelihood function is calculated from a misfit function *S(***m***)* through the following expression:

$$L(\mathbf{m}) = K \cdot \exp[-S(\mathbf{m})], \qquad\qquad \textbf{Equation 2}$$

where

K - a normalisation constant.

The probability density *p(***m***)* with a mean at $\mathbf{m_{init}}$ describes a priori information we have on the model parameters:

$$p(\mathbf{m}) = K_0 \exp\left(-\frac{1}{2}(\mathbf{m} - \mathbf{m_{init}})^T \mathbf{C_p^{-1}}(\mathbf{m} - \mathbf{m_{init}}) \right), \qquad \textbf{Equation 3}$$

where

$\mathbf{C_p}$ – parameter covariance matrix.

On each step of the Metropolis algorithm we calculate *p(*$\mathbf{m_{new}}$*)* and *p(*$\mathbf{m_{old}}$*)*, where the $\mathbf{m_{old}}$ – parameter values accepted on a previous step and $\mathbf{m_{new}}$ – a vector of new randomly chosen parameter values. The decision if the $\mathbf{m_{new}}$ is accepted is being made in two steps:

1. If *p(*$\mathbf{m_{new}}$*)*> *p(*$\mathbf{m_{old}}$*)* – the new parameter values are closer to the initial guess than the old values then the model is run with $\mathbf{m_{new}}$ and the *L(*$\mathbf{m_{new}}$*)* is calculated;

2. If *L(*$\mathbf{m_{new}}$*)*>*L(*$\mathbf{m_{old}}$*)* – the new parameter guess provides a better fit between the modelled and observed fluxes. The $\mathbf{m_{new}}$ is accepted, $\mathbf{m_{old}} = \mathbf{m_{new}}$ and new parameter values will be generated.

We assume that the model parameters initially have uniform distribution and are independent. Matrix $\mathbf{C_p}$ is diagonal (has zero values for elements off the diagonal) with the parameters variances as diagonal elements. We calculate the parameters variances from available measurements from the work of White et al. (2000) as well as the upper and lower bounds $\mathbf{B_{up}}$ and $\mathbf{B_{lo}}$ for each parameter to restrict the optimisation routine to sample only ecologically sensible parameter values, for example, to sample only positive values for carbon pools.

Misfit function

The misfit function is a function of model parameters which gives a measure of match between model predictions parameterised with set **m** and the observations:

$$S(\mathbf{m}) = \frac{1}{2}(\mathbf{D_{cal}} - \mathbf{D_{obs}})^T \mathbf{C_f^{-1}}(\mathbf{D_{cal}} - \mathbf{D_{obs}}),$$ **Equation 4**

where

$\mathbf{D_{cal}}$, $\mathbf{D_{obs}}$ - matrices those M rows are vectors of model outputs or constraints, respectively.

Each model output $\mathbf{D_{cal}}[i] = \mathbf{d}^i_{cal}$ is either a vector of carbon flux values (*NEP*, *GPP* or *RESP*) or a vector of *LAI* values. The difference between the model output and the observations is defined as:

$$\mathbf{D_{obs}}[i] - \mathbf{D_{cal}}[i] = \mathbf{d}^i_{cal} - \mathbf{d}^i_{obs} = \frac{1}{N-1}\sum_{j=0}^{N-1}\left(d^i_{cal}[j] - d^i_{obs}[j]\right)^2,$$ **Equation 5**

where

i – row index from 0 to M-1,

N - number of elements in each of the model outputs (N = 365 days of year).

Similarly as for the model parameters, we assume that the model outputs are independent from each other. The covariance matrix $\mathbf{C_f}$ is diagonal, where each element of $\mathbf{C_f}[i, i]$ is an expected value of $\mathbf{D_{cal}}[i]$ - $\mathbf{D_{obs}}[i]$, derived from previous model runs.

The day-to-day fluctuations of carbon fluxes and *LAI* calculated by the model and their observations change over the year and have higher amplitudes in summer than in winter. If we calculate the misfit function between the measured and the modelled fluxes straight forward, the contribution to the misfit value provided by summer carbon fluxes will be larger than by the winter fluxes. This would lead the optimisation algorithm to minimise largest misfits in summer fluxes while the fitting during winter time will remains loose. To avoid this effect we apply a weighting function to the measured ($\mathbf{flux}^i_{obs}$) and modelled ($\mathbf{flux}^i_{obs}$) fluxes. To give equal significance to the winter and summer fluxes the *log* transformation was applied to elements of $\mathbf{flux}^i_{obs}$ and $\mathbf{flux}^i_{obs}$:

$$\mathbf{d}^i_{cal}[j] = \log\left(\mathbf{flux}^i_{cal}[j] + SH\right)$$ **Equation 6**

$$\mathbf{d}^i_{obs}[j] = \log\left(\mathbf{flux}^i_{obs}[j] + SH\right),$$ **Equation 7**

where

SH - normalisation constant that ensures the argument of *log* function is a positive number.

The uncertainty of model output

A priori uncertainty of the model output is calculated by running the model with parameter values sampled within initially defined parameter ranges. In order to obtain a posterior

estimation of the model output uncertainty the model is run with parameter values varying within the posterior ranges, which were determined by the optimisation procedure.

For the quantitative estimation of the model output uncertainty we introduce a new variable *UNCERT*. *UNCERT* is a measure of a difference between the upper ($d^i_{975}[j]$) and the lower ($d^i_{025}[j]$) bounds of the model output at the time step *j* that correspond to the 97.5% and 2.5% quintiles of all sampled $d^i_{cal}[j]$:

$$UNCERT = \frac{1}{(M-1)(N-1)} \sum_{i=0}^{M-1}\sum_{j=0}^{N-1} \left(d^i_{975}[j] - d^i_{025}[j]\right)^2 \qquad \textbf{Equation 8}$$

Comparing the values of *UNCERT* for different sets of parameters we can quantify the success of the performed parameter optimisation. If the *UNCERT* value computed with the posterior parameter values is smaller than *UNCERT* calculated with a priori parameter values, we conclude that the flux uncertainty has been reduced and the optimisation was successful. Otherwise the optimisation did not improve the simulated carbon fluxes with the given parameter set. The *UNCERT* was calculated for all six sites with initial and with optimised parameter values and the relative change in the *UNCERT* value after the optimisation.

One iteration of the optimisation

At each step of the parameter optimisation routine new parameter values **m_new** are sampled. The parameter values **m_new** used for the first model run – the spinup run. After the spinup run is completed, the carbon, nitrogen, and water pools state is saved into a restart file. The restart file is then used in the subsequent normal run. A more detailed scheme of the iterative algorithm can be seen in the Figure 12:
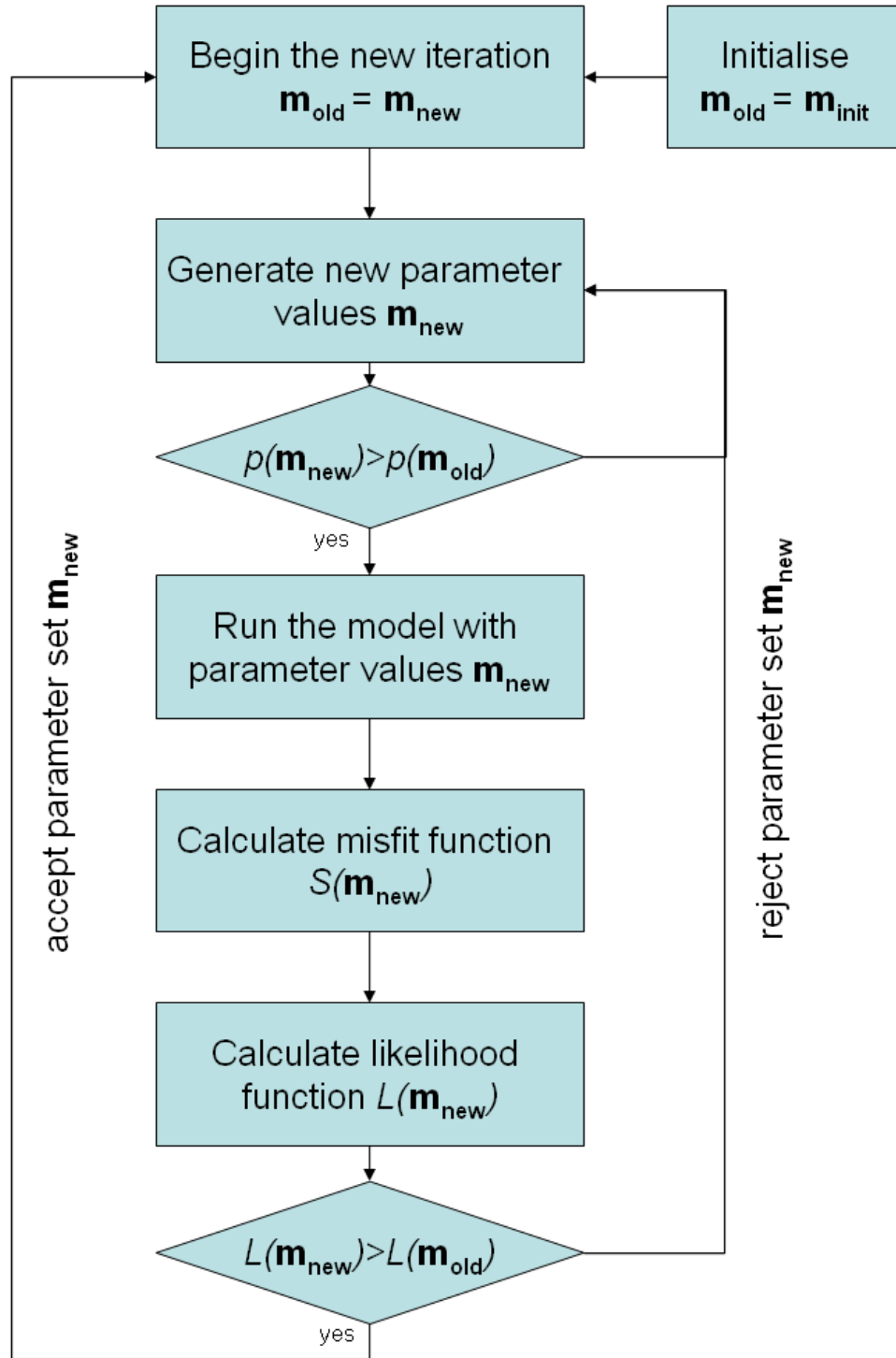
Figure 12. Scheme of the iterative optimization algorithm.

Constraints on the model output

We use multiple independently measured constraints on the model output at the sites: the *NEP* flux and the maximum annual *LAI*. We use the ecosystem respiration (*RESP*) and *GPP* inferred from the *NEP* measurements (Reichstein et al., 2005) to constrain the modelled ecosystem respiration and photosynthesis, respectively.

We run the optimisation procedure with four different combinations of constraints for the study sites, named RUN_A, RUN_B, RUN_C, and RUN_D with the $CONSTRAINTS_A$, $CONSTRAINTS_B$, $CONSTRAINTS_C$, and $CONSTRAINTS_D$, respectively (Table 11). The posterior parameter values derived in RUN_A, RUN_B, RUN_C, and RUN_D were named $VALUES_A$, $VALUES_B$, $VALUES_C$, and $VALUES_D$, respectively.

Table 11. Different combinations of constraints used in the model parameter optimisation procedure.   Constraints marked by symbol „+"are included into a corresponded combination.

Combination code	Constraints				Output
	NEP	*GPP*	*RESP*	*LAI*	
$CONSTRAINTS_A$	+				$VALUES_A$
$CONSTRAINTS_B$			+		$VALUES_B$
$CONSTRAINTS_C$			+	+	$VALUES_C$
$CONSTRAINTS_D$		+	+	+	$VALUES_D$

Results and Discussion

Model output calculated with the initial parameter values matched seasonal trends of the measured carbon fluxes and *LAI*, but the summer *GPP* was underestimated for all study sites. The *LAI* calculated by the model agreed well with the measurements for all sites. For coniferous sites the *NEP* and *RESP* fluxes were overestimated by the model. For deciduous sites the *RESP* flux was overestimated during the growing season but the calculated *NEP* matched observations fairly well. For coniferous as well as for the deciduous sites the model parameters had to be adjusted in a way to reduce the *RESP* flux and still provide match of *GPP* and of *LAI* to the measurements.

Firstly, we analysed which observations or which combinations of them provide better constrain of the model parameters. Secondly, prior and posterior parameter confidence intervals were analysed. The magnitude of the reduction of each parameter's confidence interval was interpreted as the efficiency of the optimisation procedure with the respective input constraints for this parameter.

Uncertainty in carbon fluxes

Hyytiala and Soroe. For Hyytiala and Soroe all applied constraints combinations reduced uncertainty in modelled carbon fluxes and *LAI* (Table 12). For these sites all considered sets of constraints contained additional information about carbon budget, this information was not controversial, and provided a more accurate estimation of model output and model parameters than the initial parameter set. The $CONSTRAINTS_D$ helped to reduce the uncertainty of a larger number of model parameters: canopy specific leaf area was constrained by adding of the *LAI* and *GPP* observations. Thus, the $CONSTRAINTS_D$ was the most efficient constraint on the model output and parameters for these two sites.

Table 12. Relative change in the flux uncertainty measure (*UNCERT*) propagated by optimisation with different sets of constraints applied to model output. Negative values indicate reduction of the flux uncertainty; positive values show an increase in flux uncertainty. Shading of cells indicates that uncertainty (*UNCERT* value) of all model outputs (*NEP*, *GPP*, *RESP*, and *LAI*) was reduced.

| Site | Flux | Reduction of the *UNCERT* in percent from initial value | | | |
		$CONSTRAINTS_A$	$CONSTRAINTS_B$	$CONSTRAINTS_C$	$CONSTRAINTS_D$
HA	*NEP*	-24.46	-15.12	-9.19	-57.87
	RESP	-21.97	156.08	-33.34	-70.89
	GPP	-25.51	14.05	7.68	-50.88
	LAI	-41.18	-88.45	-94.79	-84.81
HE	*NEP*	68.60	7.16	70.76	-4.59
	RESP	-41.92	-40.97	58.95	140.38
	GPP	90.38	-32.64	168.32	-15.96
	LAI	-24.91	-61.63	-64.40	-78.65
SO	*NEP*	-52.40	-41.35	-21.24	-22.30
	RESP	-87.19	-8.97	-58.35	-70.22
	GPP	-62.52	-48.09	-35.71	-36.71
	LAI	-63.40	-71.84	-93.47	-90.60
HY	*NEP*	-57.59	-48.49	-63.50	-48.57
	RESP	-71.64	-29.72	-75.61	-68.63
	GPP	-57.44	-55.66	-74.22	-50.07
	LAI	-70.88	-81.06	-89.25	-86.03
LO	*NEP*	-58.55	-3.13	-56.34	-33.46
	RESP	-79.55	95.76	-56.76	-64.05
	GPP	-77.49	-25.77	-51.41	-58.83
	LAI	-48.24	-68.70	-95.53	-85.95
TH	*NEP*	-87.85	-57.61	-67.18	-72.80
	RESP	-91.49	-65.23	-41.07	-85.19
	GPP	-90.99	-72.82	-69.68	-75.32
	LAI	-41.10	19.49	-78.49	-83.28

Loobos, Tharandt, and Hainich. For Loobos, Tharandt and Hainich the $CONSTRAINTS_B$ did not provide any improvement to the model output. It happened because only the respiration part of the carbon balance was constrained but the photosynthetic component, which was initially underestimated, was not constrained. For Hainich and Loobos sites the $UNCERT$ value of the $RESP$ flux (the constrained one) increased after the optimisation. It happened because the method "tried" to reduce the respiration flux and sampled model parameter values in a wider than initial range, but there was not enough information to constrain model parameters with this constraint alone. Adding the LAI constraint ($CONSTRAINTS_C$) for Hainich did not reduce the uncertainty in the model output: the GPP flux was still overestimated and its uncertainty increased after RUN_C.

Hesse. For the Hesse site the single respiration constraint ($CONSTRAINTS_B$) was the most efficient in reducing the uncertainty in model outputs. $CONSTRAINTS_B$ reduced the uncertainty of $RESP$, GPP, and LAI, but not NEP. It happened because the forest of Hesse is young (approx. 36 years old in 2001), highly productive and managed. The forest stand is recovering from the last clear-cut in 1965 and the thinning in 1999 while the litter left on the ground as a result of previous management activities contributes to the ecosystem respiration flux from the canopy. The BIOME-BGC model simulates the naturally growing forest and does not include the forest management, predicting the soil respiration flux of an unmanaged ecosystem, which is lower than the measured respiration flux. Thus, it is of a greater importance to constrain the $RESP$ model output than GPP and NEP. The $CONSTRAINTS_B$ was efficient to reduce uncertainty in $RESP$, GPP, and LAI but the uncertainty of NEE was slightly increased. However, due to a strong reduction in the uncertainty of the model parameters (CNl, CNll, CNlw, and SLA) the RUN_B was considered successful and the $VALUES_B$ were taken as the optimal values of model parameters for Hesse site.

For Hainich, Soroe, Hyytiala, Loobos, and Tharandt sites the $CONSTRAINTS_A$ and $CONSTRAINTS_D$ were the most efficient to reduce the $UNCERT$ of the model output (Table 12). To decide which set of constraints was the most successful one we had to look at the parameters uncertainties. The $CONSTRAINTS_D$ provided a stronger reduction in the UNCERT for the modelled LAI estimates and reduced the confidence intervals in a greater number of model parameters than the $CONSTRAINTS_A$ (the SLA parameter was constrained by $CONSTRAINTS_D$, but not by $CONSTRAINTS_A$). Given that the $CONSTRAINTS_D$ were more efficient than $CONSTRAINTS_A$ in narrowing the confidence intervals of optimised model parameters the $VALUES_D$ was chosen to be the optimal values of the model parameters (Table 13) for Hainich, Soroe, Hyytiala, Loobos, and Tharandt sites.

Table 13. Initial and actual (derived with *CONSTRAINTS$_D$*) parameter values and their ranges for deciduous broadleaf and evergreen needleleaf forests. The actual values of model parameters are averaged parameter values derived for individual sites. The shading of the lines indicates the parameters whose confidence intervals were redefined, but the mean values were fixed at their initial values because during the optimisation no general trend of the parameter change was found.

Parameter	initial value	a priori 95% confidence interval	optimised value	a posteriori 95% confidence interval
Decidious broadleaf forest				
CNl	24.0	16.3-35.7	20.1	13.0-27.2
CNll	49.0	16.3-114.0	66.3	32.1-100.0
CNfr	42.0	25.0-75.8	46.0	25.3-66.7
CNlw	50.0	25.0-76.0	50.0	19.0-50.9
SLA	30.0	16.3-66.7	30.0	23.2-40.3
Evergreen needleaf forest				
CNl	42.0	22.8-70.0	42.0	26.3-59.5
CNll	93.0	49.0-143.0	100.5	61.8-139.2
CNfr	42.0	27.6-200.0	86.0	26.7-145.3
CNlw	50.0	28.0-200.0	79.5	19.9-139.1
CNdw	729.0	212.0-1400.0	811.3	349.6-1273.1
SLA	12.0	2.0-21.0	10.4	7.2-13.6

After analyzing uncertainties of model outputs from the initial model run and the runs *RUN$_A$*, *RUN$_B$*, *RUN$_C$*, and *RUN$_D$*, we found that the set *CONSTRAINTS$_B$* for Hesse and the *CONSTRAINTS$_D$* for Hainich, Soroe, Hyytiala, Loobos, and Tharandt sites were the most efficient sets of observations for constraining model outputs and parameters.

Optimised parameter values

The *VALUES$_B$* for Hesse and the *VALUES$_D$* for Hainich, Soroe, Hyytiala, Loobos, and Tharandt forest stands were taken as optimised posterior estimations of model parameters. The corresponding constraint sets were the most efficient ones for the respective sites.

Estimations of confidence intervals for C:N ratio of leaves, C:N ratio of leaf litter, and SLA were reduced by the optimisation by more than 18% from initial estimations for all study sites (Figure 13 and Figure 14). For ENF sites the estimation of the confidence interval for C:N ratios of life and dead wood were reduced by more than 30% and 20% respectively from initial values. For DBF sites the confidence interval of C:N ratio of life wood was reduced by 37% from the initial value.

Deciduous Broadleaf Forest sites. For DBF sites new estimations of parameter values of CNll, CNfr, CNlw, CNdw, and SLA were found after the optimisation (Table 13). The lifetime of the deciduous broad leaves is less than one year and the leaves are the first tree-

part to react to changes in the nitrogen deposition from the atmosphere. Because the nutrient use efficiency for the leaves at DBF sites was decreased (leaves have less carbon per unit of nitrogen - CNl decreased) we conclude that the DBF sites did not experience nitrogen-limitation. The new CNl value for DBF sites defined as 20.1 matched the observed value at Hesse (21.5) better than the initial value (24.0).

The increased CNll parameter characterises the combined effects from the reduced nutrient use efficiency of the leaves and increased retention of carbon in leaf litter in attempt to reduce ecosystem respiration.

The increase of the fine roots C:N ratio was explained by the optimisation's attempt to decrease the ecosystem respiration, so there would be more carbon per unit of nitrogen in fine roots available for the autotrophic respiration.

For Hainich, Hesse, and Soroe parameters CNlw and SLA were diverging from their initial value differently:

- CNlw reduced at Hainich and Hesse, while increased at Soroe,
- SLA increased at Hesse and reduced at Hainich and Soroe.

Thus the CNlw and SLA optimised values can not be taken the general parameterisationof the DBF plant functional type. However, the newly defined confidence intervals for these parameters can be used in the future.

Evergreen Needleleaf Forest sites. For ENF sites new estimations of parameter values of CNll, CNfr, CNlw, CNdw, and SLA were found after the optimisation (Table 13). After the optimisation, SLA of coniferous forests was reduced from 0.012 m^2 kg^{-1} to 0.010 m^2 kg^{-1}, which was still higher than measured SLA of 0.004 m^2 kg^{-1} available from Tharandt. Since we do not know how representative the single measured SLA was, we conclude that our method showed at least a correct trend towards a lower than initially estimated SLA value. Since leaves with lower SLA utilise high irradiance more efficiently and are more tolerant to nutrient deficiency and drought, the simulated coniferous forests with optimised SLA produced higher *GPP*.

The optimised CNl value increased for Hyytiala and Tharandt sites but reduced for the Loobos site. These site-specific controversial changes allow us to conclude that no better general value for CNl was found. However, the CNl confidence interval was better defined.

For some parameters the posterior estimations of their means were not in the middle of their posterior confidence intervals. It implies that distributions of these parameter values had a skewed rather than Gaussian shape as we assumed initially (for example, the CNlw and CNdw parameters for DBF in Figure 13 or LWPs parameter for ENF sites and Figure 14).
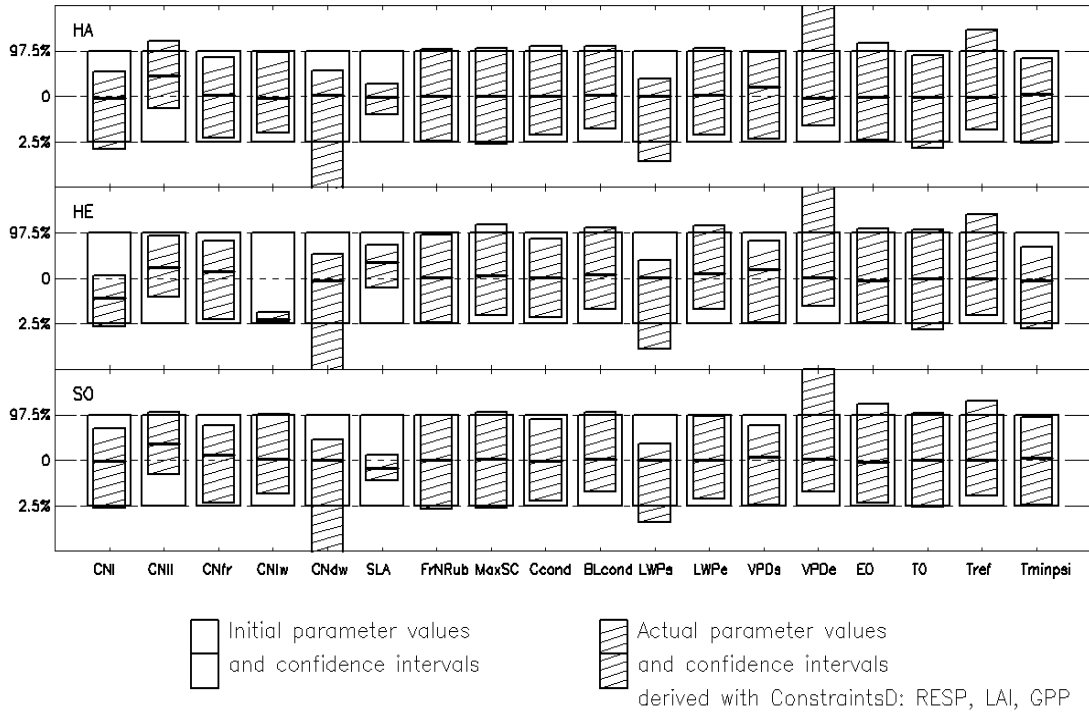
Figure 13. Mean values and 95% confidence intervals of model parameters for deciduous broadleaf sites. A plain rectangular shows the initial 95% confidence interval of a respective model parameter. The "0"- line represents initial parameter values. Each hatched rectangular shows the actual 95% confidence interval of a respective model parameter and the horizontal black bar indicates its actual value. The size of the confidence interval bars and parameter values are normalised to their initial values.

Our results showed that uncertainty of only a few of parameters included into the optimisation reduced (confidence intervals were narrowed) and their estimations were improved. In many cases the "improvement" was only site specific and could not be used to for the general parameterisation of ENF and DBF plant functional types for the BIOME-BGC model.
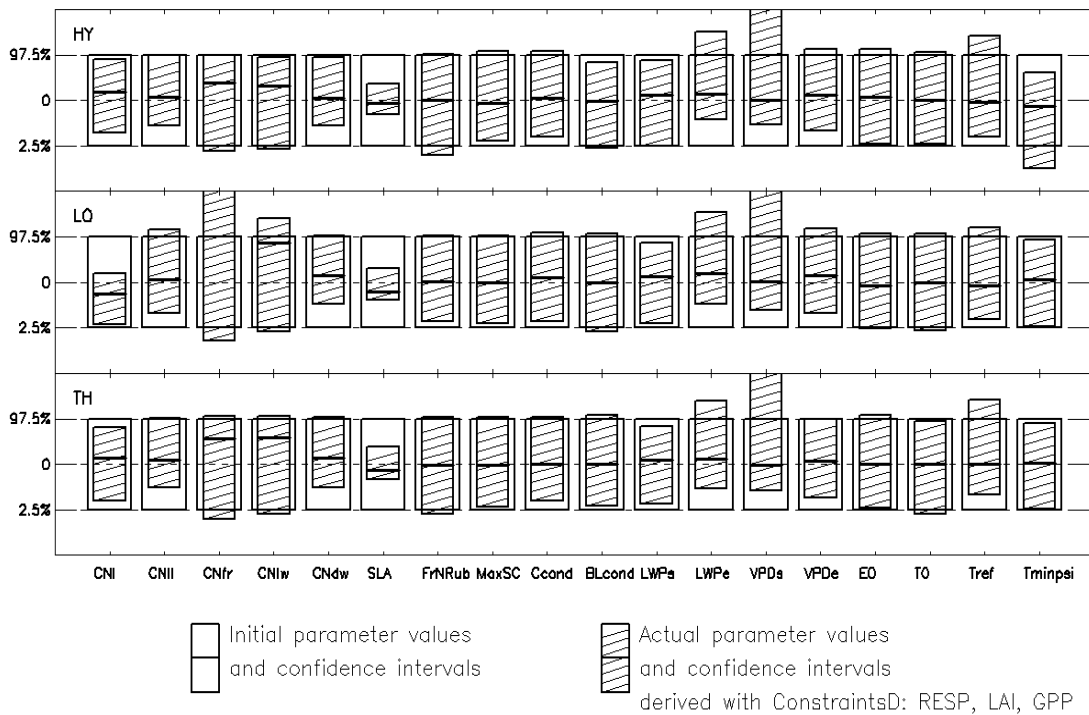
Figure 14. Mean values and 95% confidence intervals of model parameters for coniferous needleleaf sites. A plain rectangular shows the initial 95% confidence interval of a respective model parameter. The "0"- line represents initial parameter values. Each hatched rectangular shows the actual 95% confidence interval of a respective model parameter and the horizontal black bar indicates its actual value. The size of the confidence interval bars and parameter values are normalised to their initial values.

The model performance with the new estimates of model parameters was tested for two sites, which were not included into the optimisation. We calculated the daily average *GPP* flux for two forest stands – a deciduous broadleaf forest at Le Bray (France) and an evergreen needleleaf forest at Vielsalm (Belgium) and compared them to the initial flux estimates.

Testing optimised parameters

We use the optimised model parameters values for two sites Le Bray (ENF, South-West of France) and Vielsalm (DBF, Belgium) to test our assumption about a possible spatial extrapolation of our results: the new actual parameter values should improve flux estimations for other eddy-covariance measurement sites, not only for those sites which were used in the optimisation.

For Le Bray and Vielsalm sites we performed model simulations with the initial and the optimised parameter values and correlate the calculated *GPP* flux to the measurements. For these simulations we used not the meteorological measurements on the stations but the

averaged climate fields derived from the NCEP Reanalysis dataset for 0.25×0.25° footprints around the stations. Bu using the averaged meteorological data and the site-optimised model parameters we intended to demonstrate that the optimised parameters improve not only the site-specific but the general model's performance. It is important to note that the parameters optimised for conifer forests in the north-western Europe also improved the model performance for Le-Bray, which has the typical Mediterranean climate.

For Le Bray and Vielsalm sites the *GPP* flux calculated with the optimised parameters showed a better correlation with the measurements than the flux calculated with the initial parameter values. The correlation coefficients changed from 0.83 to 0.84 and from 0.71 to 0.72 for Le Bray and Vielsalm, respectively.

The average daily *GPP* at Le Bray was measured at 3.4 kgC m^{-2}day^{-1}. The modelled estimation accounted for 2.85 kgC m^{-2}day^{-1} with the initial and for 2.95 kgC m^{-2}day^{-1} with the optimised parameters.

The average daily *GPP* at Vielsalm was measured at 3.3 kgC m^{-2}day^{-1}. The modelled estimation accounted for 2.97 kgC m^{-2}day^{-1} with the initial and for 2.98 kgC m^{-2}day^{-1} with the optimised parameters.

This improvement of the flux estimations shows that the parameter values derived for other sites using site-specific meteorological data were also suitable for other sites with averaged meteorological data. This proofs our assumptions that the site-specific optimisation of model parameters may

- help to improve general parameterisation of the ecophysiological characteristics for different plant functional types,
- help to improve the performance of the model on the regional scale.

Reduction of flux uncertainty with optimised parameters

We calculate the prior and posterior uncertainty in the modelled fluxes using the initial and the optimisation-retrieved estimates of the parameter confidence intervals, respectively. We assume that the randomly sampled within their confidence intervals parameters produce the spectrum of model outputs that can be statistically analysed. We calculate distances between the 0.975 and 0.025 quantiles of 1000 model realisations at each time of model output; the average over all these distances is the "average distance" or the "uncertainty of model output".

We analyse the ratio between the model uncertainty calculated with the initial confidence intervals of model parameters (D_{init}) and the model uncertainty calculated with the optimisation-retrieved confidence intervals of these parameters (D_{optim}). As the optimisation algorithm uses flux information to constrain the model, the uncertainty of fluxes is expected to

reduce and the ratio D_{init}:D_{optim} to be less than 1. A stronger reduction of the D_{init}:D_{optim} ratio indicates the higher efficiency of the optimisation algorithm for the given site. The Figure 15 shows the normalised prior and the posterior uncertainty of the *NEE* flux. The comparison of D_{init} and D_{optim} shows that constraining model parameters helped to reduce uncertainty of the model output; the most efficient reductions were found for HA, SO, and HE sites.

Figure 15. The prior D_{init} (blue) and the posterior D_{optim} (red) uncertainty of the modelled *NEE* flux for the six optimisation sites (HA, HE, SO, HE, LO, and TH) and one additional site at Lavarone (LA), Italy. The magnitude of D_{init} was scaled to 1 and the magnitude D_{optim} is shown relative to D_{init}.
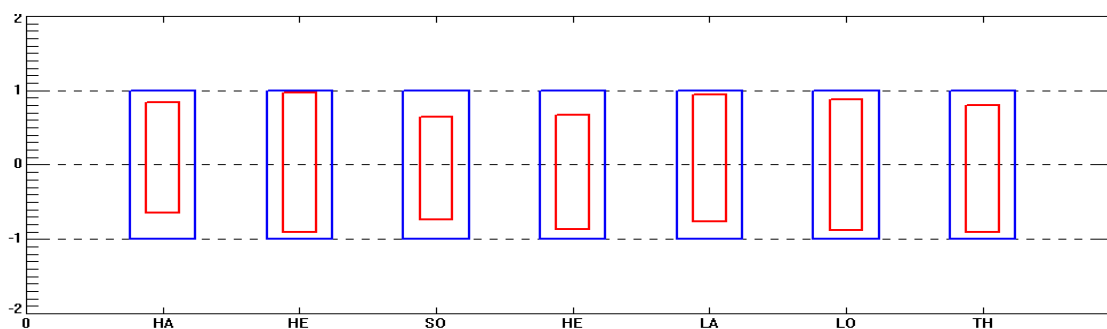
Conclusions

Testing the efficiency of the multiple constraint approach, several combinations of observations of different nature (carbon fluxes and *LAI*) were used to determine most efficient constraints on the model output and the most critical parameters for the model calibration. Suggested optimisation procedure helped to determine a set of parameters which can be constrained using the available observations for two forest types. Specific leaf area and carbon to nitrogen ratios of different parts of the forest ecosystem were the best constrained parameters.

We suggest that the improved general model parameterisation would also lead to better model estimates of regional and continental carbon budgets of forests. The test at two sites, which were not included into the optimisation, showed a better fit between the calculated and measured *GPP* fluxes. Further testing of the optimised parameters at a larger number of forest sites of different ages would be beneficial once the data are available. This would add credibility to the derived parameters and help to understand associated uncertainties.

For five out of six study sites the combination of three constraints (*LAI*, *RESP*, *GPP*) to the model output helped to reduce uncertainties of simulated carbon fluxes and *LAI* as well as of

model parameter uncertainties. Other combinations of a lower number of constraints (single *NEP*, *RESP*, or *RESP* and *LAI*) lead to some site-specific improvements of parameter estimations and flux uncertainty reduction: for Hesse site with young re-growing forest the single constraint on the soil respiration helped to obtain the best match between the model output and the observations. The improvement of model output at Hesse was less efficient than for sites with older forests. This finding points to the great importance of the respiration processes in the carbon balance of young forest ecosystems. Failure of multiple constraints to improve the model predictions at Hesse suggest that the model's general assumption about the balance between different components of the carbon balance does not hold for re-growing forests. However, at regional to continental scales simulations of uneven aged forests become less feasible because the information on management history is scarce. At these scales we most likely have to continue using the assumption about the forests being at a steady state and learn how to estimate uncertainties associated with this assumption.

Even though some model parameters are measured in the field, these measurements can not be always directly used for model parameterisation. The meanings of the measured and modelled parameters could be different. For example a definition of leaf litter can be different in the model and during sampling campaign, as a result the C:N ratio of modelled leaf litter can be quite different. One also has to pay attention to what part of ecosystem the measurement represents: SLA values measured at a few trees may not necessarily match SLA model parameter optimised with carbon fluxes for the whole forest ecosystem.

For simulations of carbon budget in Europe with the spatial version of the model BIOME-BGC we propose to use the new values of model parameters derived in this study for the deciduous broadleaf and coniferous needleleaf forests. In order to derive better estimates of ecophysiological parameters for other plant physiological types the suggested optimisation routine may be used in the future.

Acknowledgments

References

Aber, J. D. and Federer, C. A. 1992. A Generalized, Lumped-Parameter Model of Photosynthesis, Evapotranspiration and Net Primary Production in Temperate and Boreal Forest Ecosystems. *Oecologia* **92**, 463-474.

Aradottir, A. L., Thorgeirsson, H., McCaughey, J. H., Strachan, I. B. and Robertson, A. 1997. Establishment of a black cottonwood plantation on an exposed site in Iceland: Plant growth and site energy balance. *Agr Forest Meteorol* **84**, 1-9.

Aubinet, M., Grelle, A., Ibrom, A., Rannik, U., Moncrieff, J. and co-authors 2000. Estimates of the annual net carbon and water exchange of forests: The EUROFLUX methodology. *Advances in Ecological Research* **30**, 113-175.

Baldocchi, D. D. and Wilson, K. B. 2001. Modeling CO2 and water vapor exchange of a temperate broadleaved forest across hourly to decadal time scales. *Ecological Modelling* **142**, 155-184.

Baldocchi, D. D. and Bowling, D. R. 2003. Modelling the discrimination of (CO2)-C-13 above and within a temperate broad-leaved forest canopy on hourly to seasonal time scales. *Plant Cell and Environment* **26**, 231-244.

Bormann, F. H., Likens, G. E. and Melillo, J. M. 1977. Nitrogen Budget for an Aggrading Northern Hardwood Forest Ecosystem. *Science* **196**, 981-983.

Braswell, B. H., Sacks, W. J., Linder, E. and Schimel, D. S. 2005. Estimating diurnal to annual ecosystem parameters by synthesis of a carbon flux model with eddy covariance net ecosystem exchange observations. *Global Change Biology* **11**, 335-355.

Burger, G. 1997. On the disaggregation of climatological means and anomalies. *Climate Res* **8**, 183-194.

Chuine, I. and Cour, P. 1999. Climatic determinants of budburst seasonality in four temperate-zone tree species. *New Phytologist* **143**, 339-349.

Chuine, I. 2000. A unified model for budburst of trees. *Journal of Theoretical Biology* **207**, 337-347.

Chuine, I., Cambon, G. and Comtois, P. 2000. Scaling phenology from the local to the regional level: advances from species-specific phenological models. *Global Change Biol* **6**, 943-952.

Churkina, G., Tenhunen, J., Thornton, P., Falge, E. M., Elbers, J. A. and co-authors 2003. Analyzing the ecosystem carbon dynamics of four European coniferous forests using a biogeochemistry model. *Ecosystems* **6**, 168-184.

Cienciala, E., Kucera, J., Ryan, M. G. and Lindroth, A. 1998a. Water flux in boreal forest during two hydrologically contrasting years; species specific regulation of canopy conductance and transpiration. *Annales Des Sciences Forestieres* **55**, 47-61.

Cienciala, E., Running, S. W., Lindroth, A., Grelle, A. and Ryan, M. G. 1998b. Analysis of carbon and water fluxes from the NOPEX boreal forest: Comparison of measurements with FOREST-BGC simulations. *J Hydrol* **213**, 62-78.

Cienciala, E. and Lindroth, A. 1999. Analysis of carbon and water fluxes from the NOPEX boreal forest: comment. *J Hydrol* **218**, 92-94.

Cienciala, E. and Tatarinov, F. A. 2006. Application of BIOME-BGC model to managed forests 2. Comparison with long-term observations of stand production for major tree species. *Forest Ecol Manag* **237**, 252-266.

Falge, E., Baldocchi, D., Olson, R., Anthoni, P., Aubinet, M. and co-authors 2001a. Gap filling strategies for long term energy flux data sets. *Agricultural and Forest Meteorology* **107**, 71-77.

Falge, E., Baldocchi, D., Olson, R., Anthoni, P., Aubinet, M. and co-authors 2001b. Gap filling strategies for defensible annual sums of net ecosystem exchange. *Agricultural and Forest Meteorology* **107**, 43-69.

Glassy, J. M. and Running, S. W. 1994. Validating Diurnal Climatology Logic of the Mt-Clim Model across a Climatic Gradient in Oregon. *Ecological Applications* **4**, 248-257.

Gond, V., de Pury, D. G. G., Veroustraete, F. and Ceulemans, R. 1999. Seasonal variations in leaf area index, leaf chlorophyll, and water content; scaling-up to estimate fAPAR and carbon balance in a multilayer, multispecies temperate forest. *Tree Physiology* **19**, 673-679.

Goulden, M. L., Munger, J. W., Fan, S. M., Daube, B. C. and Wofsy, S. C. 1996. Measurements of carbon sequestration by long-term eddy covariance: Methods and a critical evaluation of accuracy. *Global Change Biol* **2**, 169-182.

Granier, A., Biron, P. and Lemoine, D. 2000. Water balance, transpiration and canopy conductance in two beech stands. *Agr Forest Meteorol* **100**, 291-308.

Hakkinen, R., Linkosalo, T. and Hari, P. 1998. Effects of dormancy and environmental factors on timing of bud burst in Betula pendula. *Tree Physiology* **18**, 707-712.

Haxeltine, A. and Prentice, I. C. 1996. BIOME3: An equilibrium terrestrial biosphere model based on ecophysiological constraints, resource availability, and competition among plant functional types. *Global Biogeochemical Cycles* **10**, 693-709.

Holland, E. A., Dentener, F. J., Braswell, B. H. and Sulzman, J. M. 1999. Contemporary and pre-industrial global reactive nitrogen budgets. *Biogeochemistry* **46**, 7-43.

Hunt, E. R., Piper, S. C., Nemani, R., Keeling, C. D., Otto, R. D. and co-authors 1996. Global net carbon exchange and intra-annual atmospheric CO2 concentrations predicted by an ecosystem process model and three-dimensional atmospheric transport model. *Global Biogeochemical Cycles* **10**, 431-456.

Hunt, E. R., Lavigne, M. B. and Franklin, S. E. 1999. Factors controlling the decline of net primary production with stand age for balsam fir in Newfoundland assessed using an ecosystem simulation model. *Ecological Modelling* **122**, 151-164.

Hunter, A. F. and Lechowicz, M. J. 1992. Predicting the Timing of Budburst in Temperate Trees. *Journal of Applied Ecology* **29**, 597-604.

Jonson, J. E., Bartnicki, J., Olendrzynski, K., Jakobsen, H. A. and Berge, E. 1998. EMEP Eulerian model for atmospheric transport and deposition of nitrogen species over Europe. *Environmental Pollution* **102**, 289-298.

Judson, O. P. 1994. The Rise of the Individual-Based Model in Ecology. *Trends Ecol Evol* **9**, 9-14.

Kimball, J. S., Thornton, P. E., White, M. A. and Running, S. W. 1997. Simulating forest productivity and surface-atmosphere carbon exchange in the BOREAS study region. *Tree Physiology* **17**, 589-599.

Knohl, A., Schulze, E. D., Kolle, O. and Buchmann, N. 2003. Large carbon uptake by an unmanaged 250-year-old deciduous forest in Central Germany. *Agr Forest Meteorol* **118**, 151-167.

Knorr, W. 2000. Annual and interannual CO2 exchanges of the terrestrial biosphere: process-based simulations and uncertainties. *Global Ecology and Biogeography* **9**, 225-252.

Kulmala, A., Leinonen, L., Ruoho-Airola, T., Salmi, T. and Waldén, J. 1998a. Air Quality Trends in Finland. Air Quality Measurements. Finnish Meteorological Institute, Helsinki, 251.

Kulmala, A., Leinonen, L., Ruoho-Airola, T., Salmi, T. and Waldén, J. 1998b. Air Quality Trends in Finland - Ilmanlaatumittauksia - Air quality measurements. *Ilmatieteen laitos*, 91.

Law, B. E., Williams, M., Anthoni, P. M., Baldocchi, D. D. and Unsworth, M. H. 2000. Measuring and modelling seasonal variation of carbon dioxide and water vapour exchange of a Pinus ponderosa forest subject to soil water deficit. *Global Change Biol* **6**, 613-630.

Lechowicz, M. J. 1984. Why Do Temperate Deciduous Trees Leaf out at Different Times - Adaptation and Ecology of Forest Communities. *American Naturalist* **124**, 821-842.

Lloyd, J. and Taylor, J. A. 1994. On the temperature dependence of soil respiration. *Functional Ecology* **8**, 315-323.

Malhi, Y., Baldocchi, D. D. and Jarvis, P. G. 1999. The carbon balance of tropical, temperate and boreal forests. *Plant Cell and Environment* **22**, 715-740.

Merganicova, K., Pietsch, S. A. and Hasenauer, H. 2005. Testing mechanistic modeling to assess impacts of biomass removal. *Forest Ecol Manag* **207**, 37-57.

Mosegaard, K. and Tarantola, A. 1995. Monte-Carlo sampling of solutions to inverse Problems. *Journal of Geophysical Research JGR - Solid Earth* **100**, 12431-12447.

Munger, J. W., Fan, S. M., Bakwin, P. S., Goulden, M. L., Goldstein, A. H. and co-authors 1998. Regional budgets for nitrogen oxides from continental sources: Variations of rates for oxidation and deposition with season and distance from source regions. *J Geophys Res-Atmos* **103**, 8355-8368.

Murray, M. B., Cannell, M. G. R. and Smith, R. I. 1989. Date of Budburst of 15 Tree Species in Britain Following Climatic Warming. *Journal of Applied Ecology* **26**, 693-700.

Newcomer, J., Landis, D., Conrad, S., Curd, S., Huemmrich, K. and co-authors 2000. Collected Data of The Boreal Ecosystem-Atmosphere Study. NASA.

Nizinski, J. J. and Saugier, B. 1988. A Model of Leaf Budding and Development for a Mature Quercus Forest. *Journal of Applied Ecology* **25**, 643-652.

Petritsch, R., Hasenauer, H. and Pietsch, S. A. 2007. Incorporating forest growth response to thinning within biome-BGC. *Forest Ecol Manag* **242**, 324-336.

Pietsch, S. A. and Hasenauer, H. 2002. Using mechanistic modeling within forest ecosystem restoration. *Forest Ecol Manag* **159**, 111-131.

Pietsch, S. A., Hasenauer, H. and Thornton, P. E. 2005. BGC-model parameters for tree species growing in central European forests. *Forest Ecol Manag* **211**, 264-295.

Pilegaard, K., Hummelshoj, P., Jensen, N. O. and Chen, Z. 2001. Two years of continuous CO2 eddy-flux measurements over a Danish beech forest. *Agr Forest Meteorol* **107**, 29-41.

Raupach, M. R., Rayner, P. J., Barrett, D. J., Defries, R. S., Heimann, M. and co-authors 2005. Model-data synthesis in terrestrial carbon observation: methods, data requirements and data uncertainty specifications. *Global Change Biology* **11**, 378-397.

Rayment, M. B. and Jarvis, P. G. 1997. An improved open chamber system for measuring soil CO2 effluxes in the field. *J Geophys Res-Atmos* **102**, 28779-28784.

Reichstein, M., Tenhunen, J. D., Roupsard, O., Ourcival, J. M., Rambal, S. and co-authors 2002. Ecosystem respiration in two Mediterranean evergreen Holm Oak forests: drought effects and decomposition dynamics. *Functional Ecology* **16**, 27-39.

Reichstein, M., Falge, E., Baldocchi, D., Papale, D., Aubinet, M. and co-authors 2005. On the separation of net ecosystem exchange into assimilation and ecosystem respiration: review and improved algorithm. *Global Change Biology* **11**, 1424-1439.

Ruimy, A., Dedieu, G. and Saugier, B. 1996. TURC: A diagnostic model of continental gross primary productivity and net primary productivity. *Global Biogeochemical Cycles* **10**, 269-285.

Running, S. W., Nemani, R. R. and Hungerford, R. D. 1987. Extrapolation of Synoptic Meteorological Data in Mountainous Terrain and Its Use for Simulating Forest Evapotranspiration and Photosynthesis. *Can J Forest Res* **17**, 472-483.

Running, S. W. and Coughlan, J. C. 1988. A General-Model of Forest Ecosystem Processes for Regional Applications .1. Hydrologic Balance, Canopy Gas-Exchange and Primary Production Processes. *Ecological Modelling* **42**, 125-154.

Running, S. W. and Hunt, E. R. 1991. Generalization of a forest ecosystem process model for other biomes, BIOME-BGC and an application for global-scale models. In: *Scaling Physiological Processes: Leaf to Globe, J. Ehleringer, and C. Field, pp. 1410158, Academic Press, San Diego*, 236.

Running, S. W. and Hunt, E. R. 1993. Generalization of a Forest Ecosystem Process Model for Other Biomes, BIOME-BGC, and an Application for Global Scale Models. In: *Scaling Physiological Processes: Leaf to Globe*. Academic Press, 141-158.

Running, S. W. 1994. Testing Forest-Bgc Ecosystem Process Simulations across a Climatic Gradient in Oregon. *Ecological Applications* **4**, 238-247.

Schimel, D. S., House, J. I., Hibbard, K. A., Bousquet, P., Ciais, P. and co-authors 2001. Recent patterns and mechanisms of carbon exchange by terrestrial ecosystems. *Nature* **414**, 169-172.

Sitch, S., Smith, B., Prentice, I. C., Arneth, A., Bondeau, A. and co-authors 2003. Evaluation of ecosystem dynamics, plant geography and terrestrial carbon cycling in the LPJ dynamic global vegetation model. *Global Change Biol* **9**, 161-185.

Tarantola, A. 1987. *Inverse problem theory: methods for data fitting and model parameter estimation*. New York, Elsevier.

Tatarinov, F. A. and Cienciala, E. 2006. Application of BIOME-BGC model to managed forests 1. Sensitivity analysis. *Forest Ecol Manag* **237**, 267-279.

Thornton, P. E. 1998. *Regional Ecosystem Simulation: Combining Surface- and Satellite-Based Observations to Study Linkages between Terrestrial Energy and Mass Budgets*. Department, University of Montana, Missoula.

Thornton, P. E., Hasenauer, H. and White, M. 2000. Simultaneous estimation of daily solar radiation and humidity from observed temperature and precipitation: an application over complex terrain in Austria. *Agricultural and Forest Meteorology* **104**, 255-271.

Thornton, P. E., Law, B. E., Gholz, H. L., Clark, K. L., Falge, E. and co-authors 2002. Modeling and measuring the effects of disturbance history and climate on carbon and water budgets in evergreen needleleaf forests. *Agr Forest Meteorol* **113**, 185-222.

Turner, D. P., Dodson, R. and Marks, D. 1996. Comparison of alternative spatial resolutions in the application of a spatially distributed biogeochemical model over complex terrain. *Ecological Modelling* **90**, 53-67.

Van Oijen, M., Rougier, J. and Smith, R. 2005. Bayesian calibration of process-based forest models: bringing the gap between models and data. *Tree Physiology* **25**, 915-927.

Vesala, T., Markkanen, T., Palva, L., Siivola, E., Palmroth, S. and co-authors 2000. Effect of variations of PAR on CO2 exchange estimation for Scots pine. *Agr Forest Meteorol* **100**, 337-347.

Vetter, M., Wirth, C., Bottcher, H., Churkina, G., Schulze, E. D. and co-authors 2005. Partitioning direct and indirect human-induced effects on carbon sequestration of managed coniferous forests using model simulations and forest inventories. *Global Change Biol* **11**, 810-827.

Wang, Y. P., R., L., Cleugh, H. A. and Coppin, P. A. 2001. Parameter estimation in surface exchange models using nonlinear inversion: how many parameters can we estimate and which measurements are most useful? *Global Change Biology* **7**, 495-510.

Waring, R. and Running, S. W. 1998. *Forest Ecosystems: Analysis at Multiple Scales*. New York, Academic Press.

White, M. A., Thornton, P. E. and Running, S. W. 1997. A continental phenology model for monitoring vegetation responses to interannual climatic variability. *Global Biogeochemical Cycles* **11**, 217-234.

White, M. A., Thornton, P. E., Running, S. W. and Nemani, R. R. 2000. Parameterization and Sensitivity Analysis of the BIOME–BGC Terrestrial Ecosystem Model: Net Primary Production Controls. *Earth Interact* **4**, 1–85.